

Graphene-Based Smart Platforms for Combined Cancer Therapy

Zhanjun Gu, Shuang Zhu, Liang Yan, Feng Zhao, and Yuliang Zhao*

The extensive research of graphene and its derivatives in biomedical applications during the past few years has witnessed its significance in the field of nanomedicine. Starting from simple drug delivery systems, the application of graphene and its derivatives has been extended to a versatile platform of multiple therapeutic modalities, including photothermal therapy, photodynamic therapy, magnetic hyperthermia therapy, and sonodynamic therapy. In addition to monotherapy, graphene-based materials are widely applied in combined therapies for enhanced anticancer activity and reduced side effects. In particular, graphene-based materials are often designed and fabricated as “smart” platforms for stimuli-responsive nanocarriers, whose therapeutic effects can be activated by the tumor microenvironment, such as acidic pH and elevated glutathione (termed as “endogenous stimuli”), or light, magnetic, or ultrasonic stimuli (termed as “exogenous stimuli”). Herein, the recent advances of smart graphene platforms for combined therapy applications are presented, starting with the principle for the design of graphene-based smart platforms in combined therapy applications. Next, recent advances of combined therapies contributed by graphene-based materials, including chemotherapy-based, photothermal-therapy-based, and ultrasound-therapy-based synergistic therapy, are outlined. In addition, current challenges and future prospects regarding this promising field are discussed.

1. Introduction


In recent years, graphene and its derivatives are emerging as new biomaterials for applications in biosensing, biomedical imaging, drug delivery, and cancer treatment, owing to their tunable structure, unique physical/chemical properties, and good biocompatibility.^[1–5] For example, graphene-based materials with unique 2D structure, large surface area, and versatile surface chemistry can be used as nanocarriers for drug delivery.^[6,7] In 2008, Liu et al. for the first time developed the nanoscale graphene oxide (GO) as a carrier for drug delivery

application.^[8,9] From then on, explorations on using graphene-based platforms to deliver various therapeutic agents for disease treatments have been booming carried out.^[10] Although many graphene-based materials have been successfully applied for the fabrication of drug delivery systems in experimental and preclinical animal models, there still exist many limitations, such as premature drug release during the systemic circulation, undesired accumulation in the healthy tissues, poor tumor penetration capacity, and uncontrollable drug release at the tumor sites.^[11–13] To overcome these limitations, one efficient way is to construct stimuli-responsive drug delivery systems, which are also termed as “smart” drug delivery systems.^[14] A smart platform responsive to endogenous or exogenous stimuli allows better localization and controlled release of payloads at desired biological compartment.^[15] Therefore, attempts to fabricate graphene-based drug delivery systems have shifted from conventional drug carrier toward the tumor microenvironment and/or intracellular signal

activated platforms, such as pH level, redox potential, or over-expressed enzymes, aiming to overcome the challenges accompanied with conventional drug delivery systems, and finally enhance the therapeutic efficacies and reduce the potential side-effects.^[11,16–23]

Apart from their capability of tumor microenvironment/intracellular signals-responsiveness, graphene-based materials also have the ability to respond to some physical stimuli, such as light,^[24,25] ultrasound,^[26,27] and magnetic field.^[28,29] These features not only endow them with the abilities to timely and spatially control drug/gene-payload release triggered by

Prof. Z. Gu, S. Zhu, Dr. L. Yan, Dr. F. Zhao, Prof. Y. Zhao
CAS Key Laboratory for Biomedical Effects of Nanomaterials
and Nanosafety
Institute of High Energy Physics
Chinese Academy of Sciences
Beijing 100049, China
E-mail: zhaoyl@nanoctr.cn

 The ORCID identification number(s) for the author(s) of this article can be found under <https://doi.org/10.1002/adma.201800662>.

Prof. Z. Gu, Prof. Y. Zhao
College of Materials Science and Optoelectronic Technology
University of Chinese Academy of Sciences
Beijing 100049, China
Prof. Y. Zhao
CAS Center for Excellence in Nanoscience
National Center for Nanoscience and Technology of China
Chinese Academy of Sciences
Beijing 100190, China

DOI: 10.1002/adma.201800662

exogenous stimuli but also make them potential in other cancer treatments including photothermal therapy (PTT), photodynamic therapy (PDT), magnetic hyperthermia therapy (MHT), sonodynamic therapy (SDT), ultrasound hyperthermia therapy (SHT), and radiotherapy (RT). For example, due to their high near-infrared (NIR) absorption ability and photothermal conversion efficiency, graphene-based materials have been widely used for PTT application.^[30–32] Very recently, some new unique characteristics of graphene have been found and developed for cancer therapy. For example, because of the good electroconductivity and thermal-conductivity, a few reports have shown that graphene can serve as a heat conducting base to elevate local temperature upon ultrasound irradiation, making it possible for SHT and SDT.^[33–37] Moreover, various functional nanoparticles can be loaded/anchored onto the surface of graphene to provide additional properties, which can be used for bioimaging and therapy of tumor. For instance, magnetic nanoparticles (usually iron oxide nanoparticles) with excellent magnetic properties are widely integrated with graphene for magnetic resonance imaging (MRI) and MHT application.^[38–41] In addition, graphene integrated with high Z materials or radionuclides have been found to be applicable in computed tomography/positron emission tomography imaging and RT enhancement.^[42] Overall, graphene-based materials not only can be engineered as the “smart” carriers for drug delivery upon various stimuli but also have a great potential as “combo” nanomedicine for combined cancer therapy. Till now, numerous preclinical and clinical studies have shown that monotherapy for cancer treatment often accompanies with limited clinical outcomes because of the tumor heterogeneity and drug resistance.^[43–45] Combined therapy, which typically refers to the simultaneous codelivery of two or more therapeutic agents or the combination of different modalities of medical treatments, has proposed to overcome such limitations because it can synergistically improve therapeutic efficiency while reducing the side effects.^[39,46,47] In recent years, owing to the unique chemical/physical properties, large surface area, and versatile surface chemistry, graphene-based materials have shown to be extremely attractive as a single platform for codelivery of multiple therapeutic agents or administration of different medical treatments in a timely and spatially controlled manner, obtaining maximum therapeutic effects through multimodal treatments.^[48,49] Moreover, accurate and effective synergistic therapies often require controlled therapy in response to different stimuli.^[50–52] Graphene-based materials are excellent candidates for this purpose, since they are highly versatile and adaptable as mentioned above. As a result, recent years have witnessed the rapid development of using graphene-based materials for stimuli-responsive codelivery of multiple therapeutic agents or coadministration of various treatment modalities to realize synergistic effects and better therapeutic outcomes.^[53–58]

Although the applications of graphene-based drug delivery systems have been summarized in the past several years,^[10,13,59–62] a review article focusing on stimuli-responsive graphene-based nanoplatform for combined cancer therapy is still rare. To this end, here, we mainly present some representative rational design and applications of graphene-based materials for stimuli-responsive drug delivery and combined cancer therapy. We begin with an overview of the general properties



Zhanjun Gu received his B.E. degree (2002) from Huazhong University of Science and Technology and Ph.D. degree (2007) from Institute of Chemistry, Chinese Academy of Science, under the direction of Prof. Jiannian Yao. He then became a postdoctoral fellow at University of Georgia. In 2009, he joined the faculty at CAS Key Lab for Biomedical Effects of Nano-materials & Nanosafety of the Institute of High Energy Physics, Chinese Academy of Science. His current research interests include nanomaterials synthesis, optical spectroscopy, and bioapplications of luminescent nanomaterials.



Shuang Zhu received her B.S. (2013) and M.S. (2016) degree at Shandong University and Seoul National University, respectively. She currently works as a research assistant under the supervision of Prof. Zhanjun Gu at CAS Key Laboratory for Biomedical Effects of Nano-materials & Nanosafety of the Institute of High Energy Physics, Chinese Academy of Science. Her research focuses on the synthesis of nanomaterials and the exploration their biosafety and biomedical applications.



Yuliang Zhao is the founder of CAS Key Lab for Biomedical Effects of Nano-materials & Nanosafety, and Professor and Deputy Director-General of National Center for Nanoscience and Technology of China. He was elected as a member of the Chinese Academy of Science in 2017. His research interests mainly include analytical chemistry, nanotoxicology, and nanomedicine.

of graphene-based materials and design principles for stimuli-responsive drug delivery and combined therapy. We then provide a thorough examination of both endogenous and exogenous stimuli used in graphene-based smart platforms. Next, we describe the recent advances of combined therapy contributed by graphene-based materials on three branches, chemotherapy, PTT, and ultrasound therapy based synergistic therapy,

in consideration that those are the most widely applied combined therapies mediated by graphene-based nanomaterials. Other newly emerging strategies based on graphene including PDT, MHT, gene therapy (GT), immunotherapy, and RT are also discussed within the text. Finally, the challenges and future perspectives in this promising field will be proposed.

2. Design of Graphene-Based Smart Platforms

2.1. Attributes of Graphene to Design Smart Platforms for Combined Therapy

The proof-of-principle design of graphene-based smart systems is to combine graphene or its derivatives with other functional and therapeutic moieties into a single platform. In general, the unique structural features and versatile physical–chemical properties of graphene and its derivatives enable their applications in combined cancer therapy. The details regarding graphene characteristics are described as follows.

2.1.1. Unique sp^2 -Hybridized Crystal Structure

In the honeycomb lattice of graphene, each sp^2 -hybridized carbon atom has four valence bonds, including one s and three p orbitals.^[63,64] On the basal plane, the hybridization of s and two p (p_x and p_y) orbitals leads to the formation of covalent σ -bonds with other neighboring carbons and the out of plane p (p_z) orbitals overlap each other to form delocalized π -bonds that are largely responsible for the extraordinary electronic properties. Besides, owing to the unique electronic properties and strong interaction between low-frequency photons and graphene ranging from infrared to terahertz frequencies,^[4,65] the absorbance of graphene-based materials extends from ultraviolet to infrared region, thus endowing them with excellent photothermal heating capability under NIR irradiation. As a result, these features not only make graphene-based materials suitable as effective photothermal agents for applications in ablation of tumors, but also endow them with the ability to respond to different stimuli like NIR^[66,67] or electric-field,^[68,69] facilitating the construction of the stimuli-responsive smart platforms for combined cancer therapy.

2.1.2. Perfect 2D Structure

The carbon layer structure of graphene is robust and inert, and all sp^2 carbon atoms are situated at the exposed surface.^[70] From the viewpoint of chemistry, the basal plane provides ample active sites and enough space to react with functional groups via conjugation reactions, or absorption of various functional moieties like hydrophobic drug molecules, DNA/RNA, or nanocrystals via hydrophobic interactions or π - π stacking to achieve “on demand” control over functionality.^[71,72] Based on this feature, graphene-based materials can be utilized as a versatile vehicle to load/graft various therapeutic molecules/nanoparticles, greatly benefiting their applications for the combinational cancer therapy (chemotherapy, PDT, etc.) and environmentally responsive features.

2.1.3. High Reactivity of the Edges

Besides the basal plane, the edges are another alternative location possessing the ability to functionalize graphene and its derivatives with unique functional groups.^[73–76] For graphene derivatives, in particular GO, bearing oxygen functional groups on their basal and edges, most of organic synthesis principles could be employed to couple a wide range of moieties and biomolecules with graphene nanosheets to endow them with abundant environmentally responsive features. Therefore, by exploiting the flexibility of the edges, various components such as peptides and targeting moieties can be conjugated to graphene for design and fabrication of tumor microenvironment and intracellular signal-activated materials for cancer therapy.

2.2. Design of Graphene-Based Smart Platforms for Combined Therapy

The state-of-the-art development of graphene-based smart platforms used in combined cancer therapy involves the combination or hybridization of graphene-based materials with functional components like nanoparticles, biomolecules, and polymers to potentiate their ability toward the smart actions stimulated by specified signals, including pH level, redox process, and light, as well as the synergistic enhancement of different therapeutic treatments. So far, “loading” and “grafting” methods are the most widely used strategies in the fabrication of graphene-based smart platforms for the combined cancer therapy.

Loading: Loading is a technique by which functional components can be noncovalently coated at the edges and the basal plane of graphene.^[72] From the standpoint of structural characteristics, graphene derivatives can be regarded as an amphiphilic aromatic-like molecules composed of a largely hydrophobic basal plane and hydrophilic edges.^[77,78] The basal plane offers a hydrophobic surface that is capable of firmly interacting with hydrophobic components via hydrophobic interactions or π - π stacking. On the other hand, hydrophilic species can noncovalently link at the edges via electrostatic interaction and hydrogen bonding.^[79] There are two methods for noncovalent loading of functional species on the surface of graphene, which are defined as “loading-to” and “loading-from” methods.

“Loading-from” method represents the process in which graphene derivatives serve as the matrix for loading functional species onto the graphene surface via hydrophobic interactions or π - π stacking.^[80–82] Due to the advantages of simplicity in operation and high efficiency, this method has been extensively employed for the fabrication of graphene-based materials with enhanced and even new features, which can be significantly modified by exogenous or endogenous stimuli to cause irreversible structure disintegration or conformation changes.

“Loading-to” method represents the process in which graphene is coated on the surface of nanoparticles to form core@shell structures or embedded into polymer matrix to form graphene–polymer composites through π - π interactions and/or hydrogen bonding.^[83–86] This method mainly involves the mixing of colloidal suspensions of graphene derivatives with the desired polymers or nanoparticles by simple stirring.

Grafting: Grafting is a technique by which organic moieties, polymers, or nanoparticles are covalently attached to the skeleton of graphene.^[87–90] In particular, GO possesses chemically reactive oxygen functional groups at its edges and basal plane.^[91] Thus, grafting is capable of endowing graphene-based materials with the responsiveness to various stimuli via the reactions of these groups.

2.3. Stimuli for Design of Graphene-Based Smart Platforms

Based on their diverse chemical and physical characteristics mentioned above, graphene-based materials can be inherently used in drug-delivery, PTT, and SDT/SHT applications. In addition, considering their easy-functionalization, graphene-based materials can be endowed with adaptive features and thus are approved to be smart systems which can be triggered to induce significant changes in their characteristics in response to both exogenous and endogenous stimuli. These stimuli can not only provide direct therapeutic effects (for example, chemotherapy or PTT), but also offer a synergistic treatment to destroy tumors via the generation of a broad range of therapeutic effects (**Figure 1**). For instance, once drugs are released upon acidic environment in tumors, exogenous triggers such as light or X-ray can simultaneously provide physically activated therapy such as PTT or RT to realize the synergistic treatment for cancers.

2.3.1. Endogenous Stimuli

Cancer-associated endogenous stimuli-responsive platforms have been gradually used to enhance various cancer treatments. For example, when constructing anticancer drugs delivery systems, endogenous stimuli can offer the ability to target the tumor microenvironment and intracellular signals to improve the intratumoral accumulation and promote the release of drugs in an “on-demand” manner.^[11,49,92–94] These cancer related physiological signals can be used as endogenous stimuli for designing graphene-based “smart” platforms. The signals which facilitate tumor targeting include acidities, high level of intracellular glutathione (GSH), overexpressed enzymes or membrane-protein makers, ATP, or hypoxia features in the cancer cells.

pH Level: In general, both blood and healthy tissues maintain a pH value ≈ 7.20 within the cells and ≈ 7.40 in the extracellular media.^[95] Due to the high metabolic activity of tumor cells, most tumors show a more acidic intracellular pH, ranging from 5.00 to 6.00 and the extracellular pH of tumor tissues is 6.50–7.00, which are lower than that of both blood and healthy tissues.^[96] Inside cancerous cells, the differences of pH among cytosol (7.40), endosomes (5.50–6.00), and lysosomes (4.50–5.00) are also considerable. Therefore, the internalized graphene-based materials with a specific responsiveness to pH level can targetedly release drug-payloads at tumor sites, avoiding the premature release of drug in healthy tissue. Molecules with weak acids or bases features are suitable components for the fabrication of pH-responsive graphene-based systems. For example, molecules contained functional groups like $-\text{COOH}$, $-\text{NH}_2$, and $-\text{SO}_3\text{H}$ can change from neutral to ionization forms,^[97]

which can dramatically alter the interaction and the affinity between the molecules with carrier. Thus, pH gradient is an efficient stimulus to trigger the drug release from pH sensitive graphene-based platforms.^[98–103]

GSH: Because of the necessity to defend the cells against reactive oxygen species (ROS), the concentration of antioxidants (such as GSH) within the cells is often higher than that in the extracellular space.^[104,105] For example, GSH concentration in tumor tissue is found to be approximately fourfold higher than that in normal cells.^[106,107] This feature can be exploited to design and fabricate graphene-based materials with the responsiveness to GSH stimulus, making them capable of avoiding premature release within circulation systems and releasing payloads only inside the tumor sites. In terms of the construction of GSH-responsive systems using graphene-based materials, organic moieties, polymers, and proteins are used to attach to graphene and its derivatives through breakable GSH-responsive linkers, such as disulfide bonds, noncovalent hydrophobic interactions, and π - π stacking, to develop GSH-stimuli systems.^[53,108–111] After being reacted with GSH, those graphene-based nanostructures can be swelled and/or disassembled to cause the release of cargos.^[112]

Enzymes: Catalyst enzymes play an important role in cell regulation such as metabolic processes.^[113,114] In general, abnormal cancerous cells are characterized by some certain overexpressed enzymes or proteins. Such phenomenon can be utilized for the fabrication of stimuli-responsive graphene-based materials. Organic moieties can be covalently linked to the surface of graphene via specific chemical bonds, which can be cleaved by enzymes overexpressed in the tumor tissues. When taken up by cancerous cells, the linkers that are sensitive to amylases, esterase, or proteases can be broken to release drug or induce toxic effect.^[115–117] The most commonly studied cancer-associated enzymes are metalloproteinases, hyaluronidase, and cathepsin B, which are favorable stimuli for tumor targeted drug release.^[118–121]

Other Biomolecules: The presence of specific biomolecules like adenosine triphosphate (ATP) or membrane-proteins within tumor cells has also encouraged the development of graphene-based platforms with specific tumor-targeting ability. In particular, ATP, as the cellular energy source and important cellular metabolite, is highly concentrated inside the cells compared with extracellular.^[122] This feature can be used for design of smart ATP-responsive platforms using synthetic ATP aptamers.^[123,124] Besides, over-expressed membrane proteins such as folic acid (FA) receptors, hyaluronic acid (HA) receptors, transferrin receptors, or tumor necrosis factors that specifically involve in the progression of tumors are utilized for tumor-specific targeting.^[125–130] Therefore, aptamers or proteins covalently attached with drug molecules can fall off the surface of graphene due to the stronger affinity with target molecules, consequently causing drug release.

Hypoxia: Due to the hostile growth and nutrient/oxygen consumption whereas inadequate oxygen supply, hypoxia is commonly seen in tumor cells.^[131] Although oxygen deficiency is fatal to healthy cells, tumor cells have adopted to survive under hypoxic conditions. However, such survival under hypoxic environment makes tumor cells resistant to most of the anticancer therapies, such as chemotherapy, radiotherapy, and PDT.^[132]

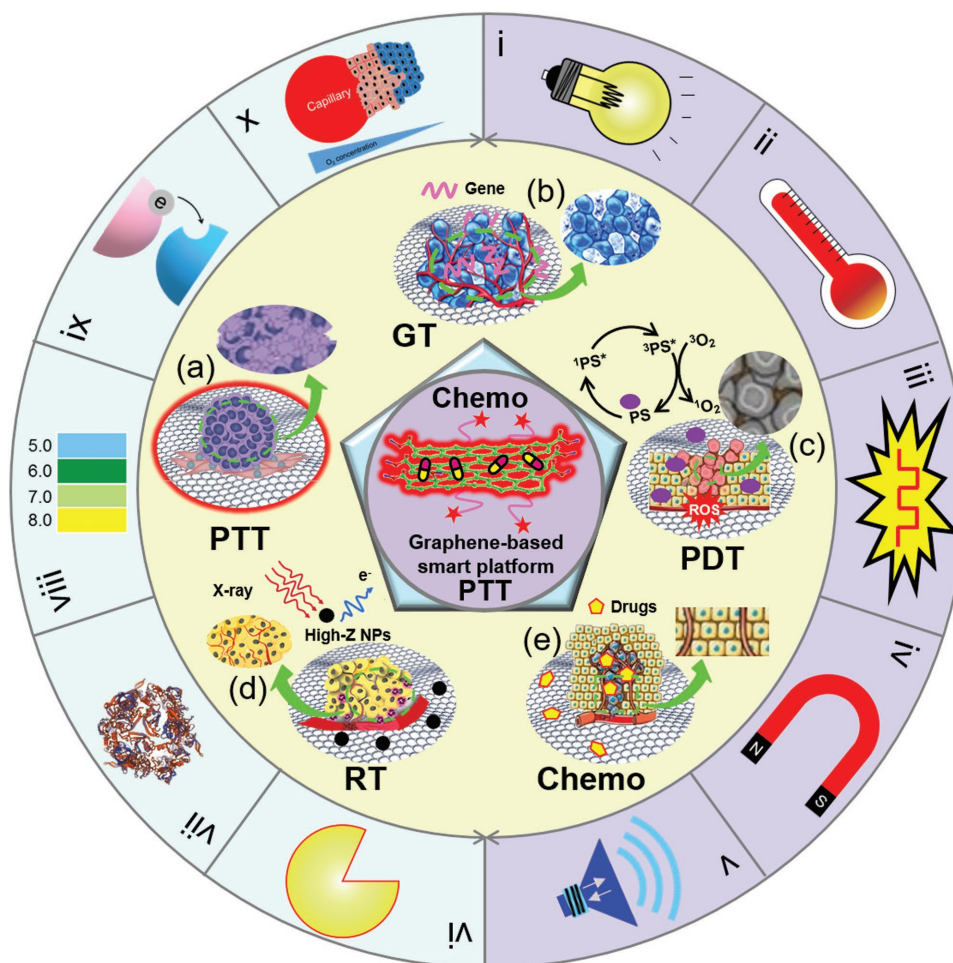


Figure 1. Schematic of a variety of stimuli to trigger the release of drugs or directly induce therapeutic effects for combined therapy: (i) light; (ii) heat; (iii) electrical field; (iv) magnetic field; (v) ultrasound; (vi) enzymes; (vii) biomolecules; (viii) pH level; (ix) redox process; and (x) hypoxia. a) Illustration of photothermal therapy (PTT). Reproduced with permission.^[239] Copyright 2013, Elsevier. b) Illustration of gene therapy (GT). Reproduced with permission.^[240] Copyright 2013, AME Publishing Company. c) Illustration of photodynamic therapy (PDT). Reproduced with permission.^[241] Copyright 2015, Brazilian Chemical Society. d) Illustration of radiotherapy (RT). Reproduced with permission.^[242] Copyright 2016, Elsevier. e) Illustration of chemotherapy. Reproduced with permission.^[243] Copyright 2017, American Association for Cancer Research.

Thus, hypoxia has been recognized as a significant target for the treatment of cancer.^[133] Graphene-based materials with large surface-to-volume ratio which can be easily functionalized to carry massive drugs are used in targeting hypoxia for tumor killing.^[134]

2.3.2. Exogenous Stimuli

In contrast to endogenous stimuli, exogenous stimuli with the aid of external physical stimuli provide powerful and effective activation pathways.^[135–137] Moreover, compared to the endogenous stimuli that are not easy to control and vary in different individuals, external physical stimuli are more reliable and efficient in the clinical practice. On the one hand, as the exogenous stimuli can offer spatial and temporal control over the activation of graphene-based smart platforms, it is proposed that toxic effects can be performed directly at the tumor sites, thus minimizing side effects in the healthy tissues. On the other hand, in addition to trigger drug release, external stimuli

such as light, ultrasound, or magnetic field can also induce additional therapeutic effects such as PTT, SDT/SHT, or MHT. As a result, the multiple responsive ability of graphene-based materials for both endogenous stimuli and exogenous physical stimuli not only benefit their smart drug delivery but also make them ideal for combined therapy of tumor.

Light: Light, as a source of energy widely used in nature, is a commonly used stimulus owing to its noninvasive nature, and the ability to fine tune the exposure location and dose.^[122] As we mentioned above, graphene has strong absorption of light in a wide range, especially in NIR region. It also possesses good photothermal conversion efficiency, making it ideal photothermal agent for photothermal ablation of tumor.^[138] Such light-induced local temperature elevation is also able to cause the release of drugs from graphene-based nanocarriers in a light-controlled manner.^[139] In addition to triggering drug release and PTT, external light is also able to stimulate graphene-based materials for PDT to destroy tumors. With the ability to carry massive photosensitizers, typical PDT can be achieved by graphene-based materials because external lights

can trigger photosensitizers to produce enormous ROS to kill cancer cells.^[5,140]

Magnetic Field: Magnetism is regarded as one of the best options for exogenous stimulus, since it almost has no physical effect on the body compared with other stimulus such as light irradiation.^[122] It thus exerts minimal adverse effects to healthy tissues. Graphene derivatives hybridized with engineered magnetic nanoparticles, such as Fe₃O₄ nanoparticles, can be magnetically controlled and driven to any part of body, and therefore become an emerging useful vehicle both in biomedical targeting and drug delivery. For example, high-gradient magnetic field has been used to guide drug to target tissue and result in high accumulation of magnetic-responsive graphene-based platforms at desired places even the total injected dose is low.^[112] In addition, graphene-based magnetic materials are also able to generate heat under the rapid rotation of the magnetic nuclei or the fluctuation of the magnetic moment, offering additional therapeutic strategy. Taken together, magnetic stimulus can be applied for targeted/controlled release of drug molecules, imaging (MRI), as well as hyperthermal therapy.^[28,29,141]

Ultrasonic: Ultrasound is a stimulus that can lead to mechanical or thermal stimulation, and has an important role in many medical applications such as bioimaging at low frequencies and the removal of tumors at high frequencies.^[142,143] When designing ultrasonic-responsive graphene-based materials, there are two key properties that are required: 1) stable drug encapsulation before applying ultrasound waves, and 2) efficient release of drug molecules in response to ultrasound waves.^[122] When ultrasounds are applied, disassembly of polymeric micelles and polymersomes can occur, resulting in the disruption of the networks and release of drugs. Furthermore, by codelivering with sensitizers, ROS can be generated under ultrasound irradiation to realize a SDT process.^[27] Due to the good electroconductivity and thermal conductivity, graphene can also function as a heat conducting base to improve local temperature under ultrasound irradiation, making them promising for SHT.^[36] The ultrasound induced SDT or SHT can focus numerous ultrasound energy onto the tumors deep situated inside the tissues and exert minimal side effects to surrounding healthy tissues.^[144] This feature greatly widens the scope of combined therapeutic strategies to increase therapeutic efficacy for tumor treatment.

3. Smart Platform for Chemotherapy-Based Combined Therapy

Numerous clinical/preclinical studies have suggested that monotherapy such as chemotherapy is not as effective as we expected, mainly due to the facts like drug resistance of cancer cells and individual differences in cancer patients.^[145,146] However, by tackling multiple targets, combined therapy, which uses more than one therapeutic approach, has shown great potential for enhancing the therapeutic effects. As chemotherapy is the first-line therapy in the clinical cancer treatment, various chemotherapy-based combination therapeutic modalities are studied in research or clinical studies. Owing to the large surface area, easiness of functionalization, and

high chemical and mechanical stability in complicated physiological environment, graphene-based materials are regarded as excellent carriers for chemotherapy-based combined therapy (Figure 2).

3.1. Platforms for Combination of Photothermal Therapy with Chemotherapy

Seeking for the best way to overcome drug resistance, which is the major barrier toward practical chemotherapy, has been the hot topic for decades.^[39,147] Several studies have shown that photothermal effects can increase the sensitivity of tumor cells to DNA damaging chemodrugs, such as doxorubicin (DOX), because the hyperthermia can interfere with DNA repair.^[148] Moreover, the NIR-induced hyperthermia is considered to enhance drug cellular uptake by increasing cell membrane permeability.^[149] In addition, it is now widely accepted that PTT can not only directly cause cancer cell death but also enhance chemotherapy efficacy, as hyperthermia can promote drug release at the tumor sites.^[43] Such light-triggered drug release in the cells can also reverse multidrug resistance mechanisms such as drug efflux.^[150,151] Thus, the combination of chemotherapy with PTT may produce extra synergistic therapeutic effects.^[58,152–155] When it comes to construct graphene-based smart platforms for dual chemo/PTT therapy, targeted drug delivery in response to tumor microenvironment (such as lower pH level or increased GSH concentration) is widely used. With such tumor-targeted ability, the therapeutic efficacy can be elevated and potential side-effects to normal tissue are consequently decreased.

Feng et al.^[100] once successfully developed an intelligent pH-responsive nanocarrier based on GO for combined chemo and PTT with an emphasis on overcoming drug resistance. In the typical design, GO was first coated with dual types of polymers, polyethylene glycol (PEG) and 2,3-dimethylmaleic anhydride (DA) modified poly(allylamine hydrochloride) (NGO-PEG-DA). Such composite could be stable and negatively charged under pH at 7.40. But once inside acidic environment, it could be quickly converted to positively charged ones with elevated cellular uptake capability. DOX was embedded inside the nanocomposite, which could be on-demand released from the nanocarriers under tumor pH (e.g., 6.80) (Figure 3). Utilizing the good photothermal conversion ability of GO, they further gave evidence of the newly synthesized nanocarriers for combined chemo/photothermal therapy with enhanced efficacy in treating drug resistance cancer cells. In addition to single pH-responsive system, Dou et al. fabricated a PVP-functionalized nanocomposite composed of reduced graphene oxide (rGO) and Bi₂S₃ (PVP-rGO/Bi₂S₃) for dual pH-responsive and NIR-responsive drug delivery system.^[156] The treatment of both cancer cells (including BEL-7402, Hela, MCF-7, and HepG2 cells) and Bel-7402 tumor-bearing mice with the as-obtained nanocomplex and NIR laser irradiation greatly inhibited the growth of tumors in comparison to the treatment with chemotherapy or PTT alone, exhibiting a synergistic elevated anticancer effect (Figure 4). Additionally, Liu and co-workers synthesized a novel GO-hybridized nanogels with dual pH-stimuli and reduction-stimuli for combined chemo/photothermal therapy.^[157]

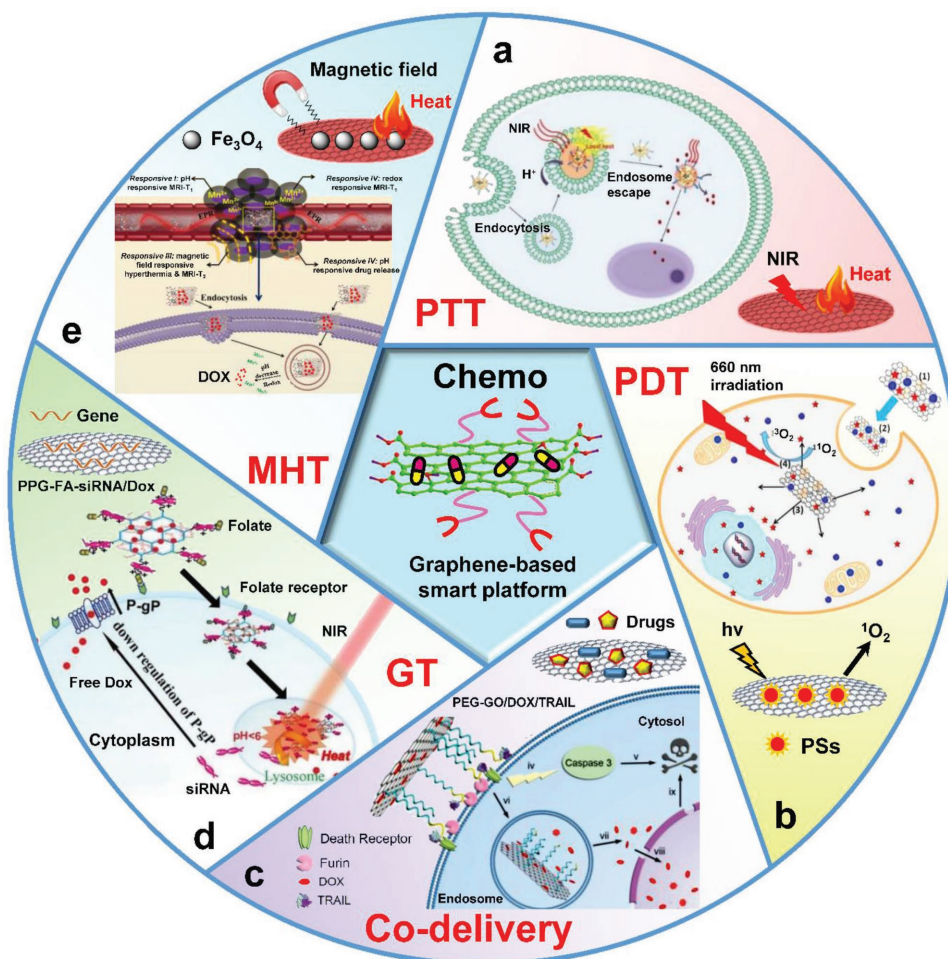


Figure 2. Schematic of graphene-based materials as excellent carriers for chemotherapy-based combined therapy. a) Combination of PTT with chemotherapy. Reproduced with permission.^[53] Copyright 2013, American Chemical Society. b) Combination of PDT with chemotherapy. Reproduced with permission.^[172] Copyright 2014, American Chemical Society. c) Codelivery of multiple anticancer drugs. Reproduced with permission.^[130] Copyright 2014, Wiley-VCH. d) Combination of GT with chemotherapy. Reproduced with permission.^[189] Copyright 2017, Springer Nature. e) Combination of MHT therapy with chemotherapy. Reproduced with permission.^[54] Copyright 2014, Wiley-VCH.

As disulfide links can be easily cleaved in the presence of GSH, this DOX-loaded novel nanogels containing disulfide cross-links showed accelerated drug release under both acidic and reducible situations (mimicking low pH and high GSH concentration), which were common conditions in tumor cells. With the excellent photothermal effects of GO, the *in vitro* cell experiments successfully proved such multifunctional nanocarriers had combined anticancer therapy effects. Moreover, Kim et al.^[53] described a trimodality responsive drug delivery and PTT using a functionalized rGO. In addition to pH-responsive and GSH-responsive, loaded-DOX could also be efficiently released by photothermal effect upon NIR irradiation. Most importantly, this nanocomplex was found to escape from endosomes and release drug within the cytosol for more killing effects due to the photothermally induced endosomal disruption. Similarly, Wang and co-workers designed and synthesized novel quadruple-responsive nanocarriers using poly(*N,N*-dimethylaminoethyl methacrylate) (PDMAEMA) modified rGO/mesoporous silica sandwich-like nanocomposites, where rGO was NIR-responsive, disulfide linker was redox (GSH) sensitive, and

PDMAEMA were pH-responsive and temperature-responsive for releasing loaded cargo molecules.^[158]

Apart from tumor pH and redox conditions, many enzymes or membrane proteins that are specifically overexpressed or malfunctioning in tumor cells are also used as targets for the enhancement of various treatments of cancer. For example, Gao et al.^[116] reported a tumor microenvironment targeted therapeutics using a NIR dye labeled-matrix metalloproteinase-14 (MMP-14) peptide substrate conjugated GO/Au complex (CPGA). As gold nanoparticles (AuNPs) possess strong NIR absorbance and surface plasmon resonance capacity, these could be used as a PTT agent and fluorescent quencher to maintain CPGA at quenched state. However, once MMP14 peptide substrate was degraded by MMP-14, an endopeptidase that was overexpressed in cancer cell membrane, fluorescent dye could subsequently provide real-time images of CPGA from whole body. Besides, the combined photon absorbance from Au/Go complex also improved PA signals compared to each single component. This work provided an enzyme triggered fluorescent/PA imaging and enhanced PTT for efficient cancer

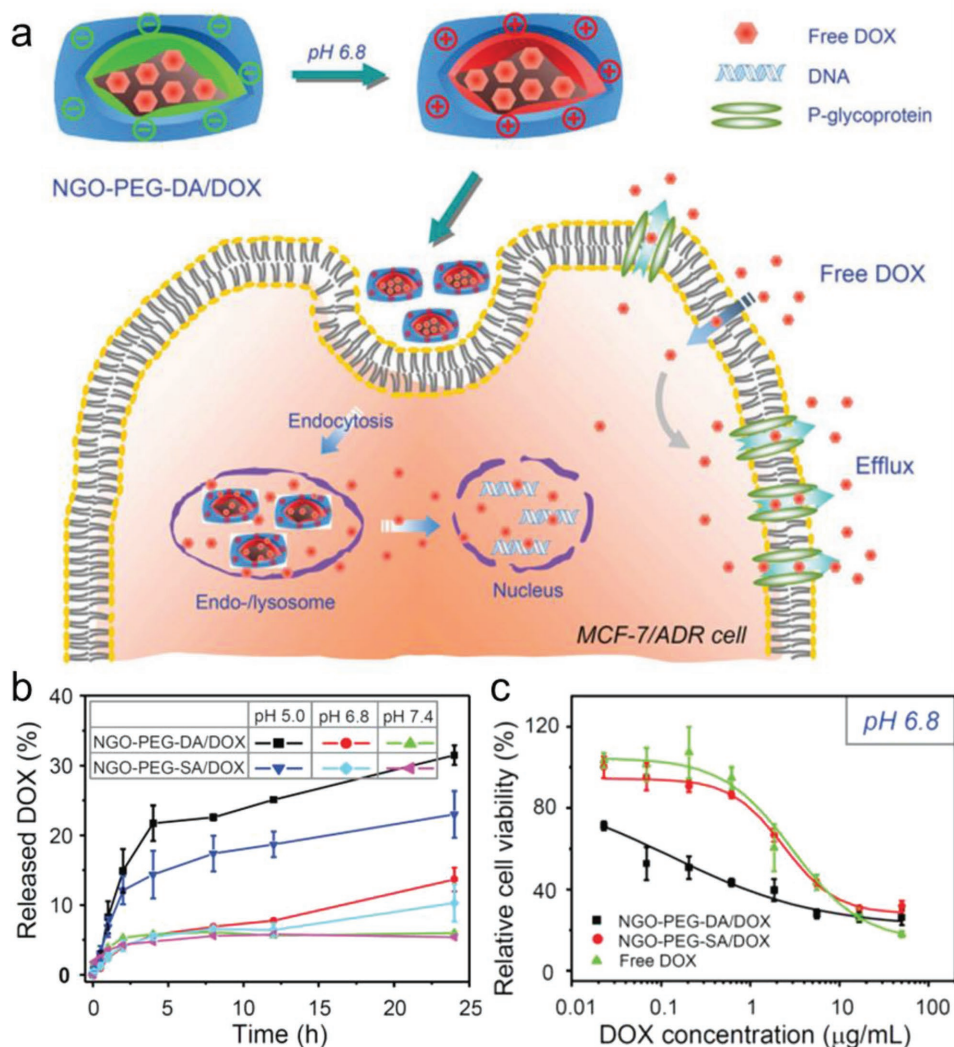


Figure 3. a) Schematic illustrations of the acidic extracellular environment-induced charge reverse of our fabricated NGO-PEG-DA/DOX complex, its cellular uptake, and intracellular acidic environment-triggered DOX release. Compared with wild-type MCF-7 cells, drug-resistant MCF-7/ARD cells with higher expression of P-glycoprotein show a rapid drug efflux. b) pH-dependent DOX release profiles of NGO-PEG-DA/DOX and NGO-PEG-SA/DOX incubated under different pH values, respectively. c) Relative cell viabilities of MCF-7/WT cells treated by NGO-PEG-DA/DOX, NGO-PEG-SA/DOX, and free DOX at pH 6.80. a–c) Reproduced with permission.^[100] Copyright 2014, Wiley-VCH.

treatment. In addition, membrane receptors such as HA receptors were also widely used for tumor-specific targeting.^[127,159–162] In 2013, Wang et al.^[152] successfully prepared a targeting peptide (IP)-modified mesoporous silica-coated graphene nanosheets (GSPI), and then introduced to the combined chemo and PTT application. As receptor chain 2 of interleukin 13 (IL-13R α 2) was widely known to be overexpressed in many malignant tumors such as glioma, the researchers therefore incorporated a natural ligand with high affinity to IL-13R α 2 into the nanocomposites. Their results indicated that the IP modification was particularly useful, as it could significantly enhance the accumulation of GSPI within glioma cells and remarkable release characteristics including heat-responsiveness and pH-responsiveness, and sustained release, finally resulting in the highest rate of death of glioma cells compared to that of single chemotherapy or PTT. In 2014, Hahn and co-workers successfully developed a transdermal GO-HA conjugate for combined

chemotherapy and PTT in melanoma skin cancer treatment.^[127] Due to the overexpression of HA receptors and leaky structures of tumor tissue, the targeted delivery of drug loaded conjugate to tumor tissue in the skin of mice was confirmed by confocal microscopy and ex vivo bioimaging. Besides, the NIR irradiation also led to complete destruction of tumor tissues with no recurrence.

3.2. Platforms for Combination of Photodynamic Therapy with Chemotherapy

PDT is a noninvasive technique for the potential use in clinical treatment of various diseases including cancer.^[163] It mainly involves the use of light with the appropriate wavelength as an exogenous stimuli to selectively activate photosensitizers at the targeted region, leading to the generation of various ROS

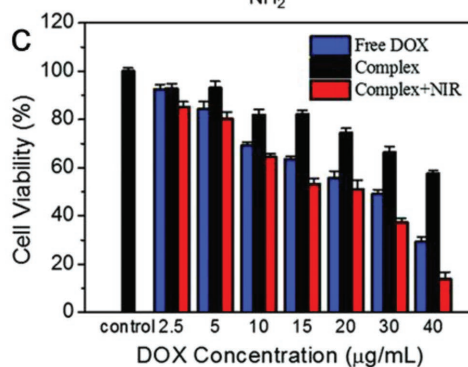
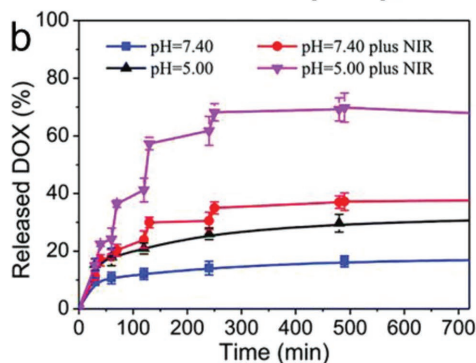
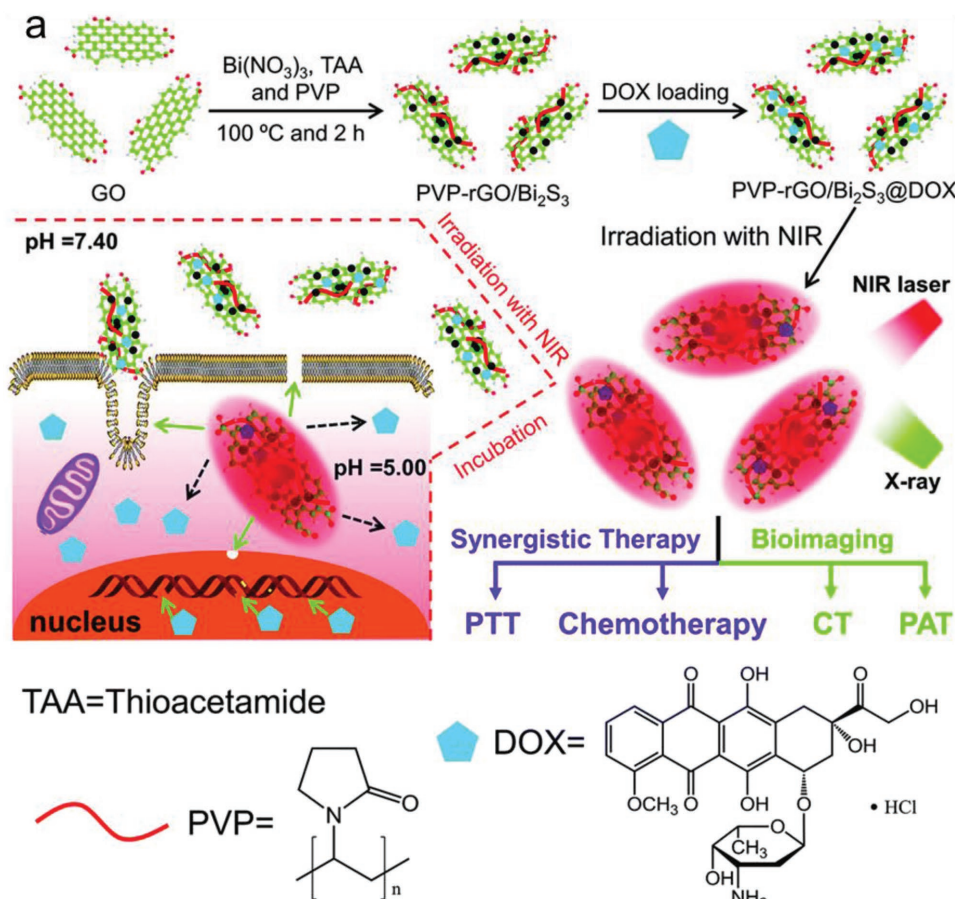


Figure 4. a) Illustration of synthesis of the PVP-rGO/Bi₂S₃ nanocomposite as well as the mechanism of combined chemo-photothermal treatment of cancer cells. b) DOX release from the PVP-rGO/Bi₂S₃@DOX complex with or without 808 nm laser irradiation at different pH values. c) Cell viabilities of HepG2 cells incubated with free DOX, the PVP-rGO/Bi₂S₃ nanocomposite, and the PVP-rGO/Bi₂S₃@DOX complex, respectively, for 24 h without or with 808 nm laser irradiation. a–c) Reproduced with permission.^[156] Copyright 2016, Royal Society of Chemistry.

like singlet oxygen (¹O₂) and hydroxyl radicals (HO[•]) to effectively kill tumor cells.^[164] Due to the massive loading capability, graphene-based materials have been used for codelivery of hydrophobic photosensitizers and tumor-specific stimuli agents for novel targeted effective PDT application.^[165–169] With the increasing need, these years, the combination of chemotherapy with PDT has also been widely studied in the preclinical tumor treatment application.^[170–173] By combining chemotherapy with PDT, ROS generated by PDT can promote intracellular drug delivery and inhibit the drug efflux

probability, while anticancer drug effect can improve the sensitivity of tumor to PDT.^[39]

In 2013, Miao et al.^[170] reported GO nanosheets based nanocarriers in a synergistic chemo/PDT for cancer treatment. GO nanosheets were grafted with PEG to enhance the biocompatibility and cellular delivery of the as-prepared nanosystems, which were then carried with photosensitizers (chlorin e6, Ce6) and DOX. Both in vitro and in vivo studies were conducted, where they found that the combination of photosensitizers and anticancer drug at a synergistic ratio could significantly enhance

the efficacy of PDT. Later, Wu et al.^[172] successfully fabricated another photoresponsive and chemoresponsive nanocomplex based on a poly-L-lysine (PLL) functionalized graphene (G-PLL). This nanoformulation was further loaded with Zn(II)-phthalocyanine (ZnPc) and anticancer drug DOX (G-PLL/DOX/ZnPc). The as-synthesized nanocomplex displayed high stability in biological solutions, high drug loading capability, pH-responsive drug release, and high ¹O₂ yield for PDT (Figure 5). The combination of PDT with chemotherapy allowed a dose reduction of anticancer drug to maximize therapeutic effects with lowered side effects.

More recently, the combination of chemotherapy with PDT/PTT is receiving more and more attention for the enhanced antitumor efficacy and reduced systemic toxicity. As a representative paradigm, Chang et al.^[174] synthesized a multifunctional rGO hydrogel as drug carriers for synergistic chemo/PTT/PDT application. In the typical design, spinach extract was used as a natural photosensitizer for tumor ablation and a biocompatibility enhancer for the hydrogel system. Gold nanocages were incorporated for PTT and at the same time enhanced the production of cytotoxic ¹O₂. Due to the large surface area and good photothermal energy conversion, rGO could offer a big platform for highly fluorouracil (5-FU) loading and photothermal enhancement (Figure 6). The resulting composite hydrogel displayed several competitive advantages, such as high drug concentration around cancer cells or excellent PDT/PTT compatibility for enhanced antitumor effects. Their study successfully demonstrated a localized and NIR-triggered combined PDT/PTT/chemotherapy based on a rGO-based platform, which exhibited remarkably improved antitumor efficacy than any single treatment.

3.3. Platforms for Codelivery of Multiple Anticancer Drugs

The combination of two or more chemotherapeutic drugs is another efficient strategy to overcome drug resistance in chemotherapy. Different drugs destroy tumors in the different pathway. Therefore, the codelivery of two or more anticancer drugs can lead to enhanced therapeutic effects due to the synergistic killing effects. For example, while drugs mainly target the nucleus to cause tumor inhibition, cytokines can target membrane proteins to trigger apoptosis to achieve synergistic anticancer therapy.^[130] In many codelivery systems, multiple therapeutics

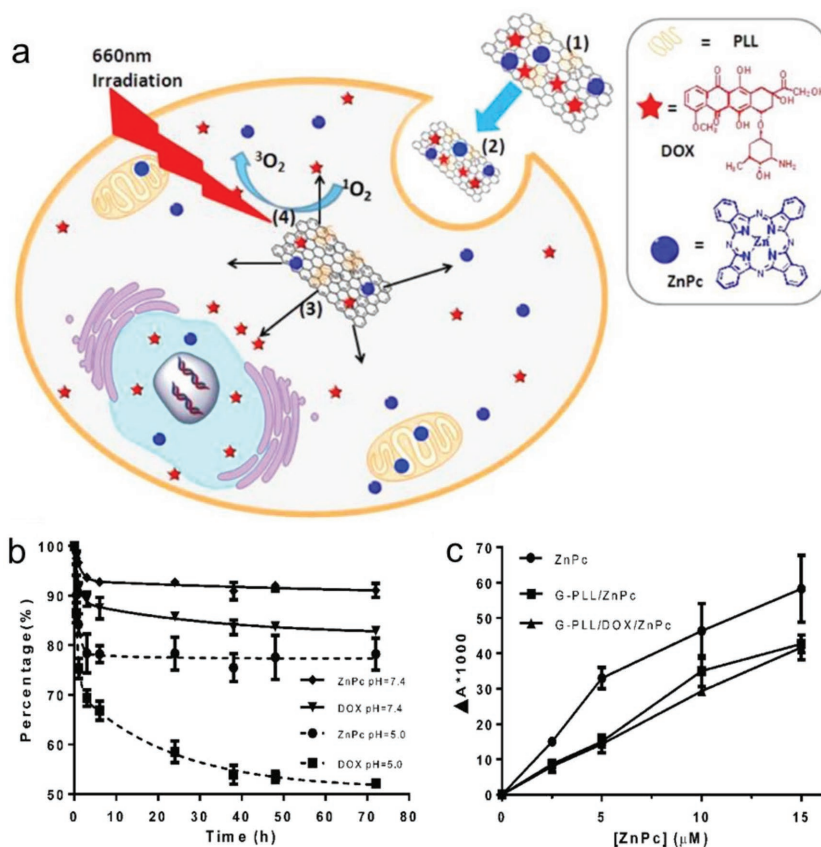


Figure 5. a) Proposed synergistic anticancer mechanism of G-PLL/DOX/ZnPc. b) Release curves of DOX and ZnPc in PBS buffer (pH = 5.0 and 7.4). c) Decrease of absorbance at 440 nm of ¹O₂ probe when incubated with ZnPc, G-PLL/ZnPc, and G-PLL/DOX/ZnPc under irradiation. PLL: poly-L-lysine; ZnPc: Zn(II)-phthalocyanine. a–c) Reproduced with permission.^[172] Copyright 2014, American Chemical Society.

can be sequentially released under different stimulus as in a programmed manner, which can further reverse drug resistance and enhance the therapeutic efficacy.^[175] In addition, dual-chemotherapy also exhibits lower side effects because of the reduced drug dose. Currently, therapeutic agents which

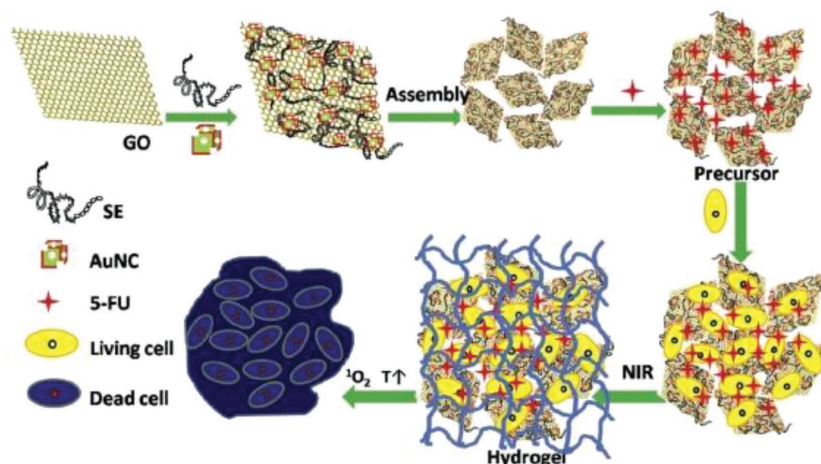


Figure 6. Illustration of the formation process, loaded with 5-FU and the antitumor mechanism of the composite hydrogel. Reproduced with permission.^[174] Copyright 2016, Elsevier.

are commonly codelivered using graphene-based materials are mainly chemodrugs, natural-inhibitors or chemoinhibitors or cytokines.^[130,176–179]

In 2016, Muthoosamy et al.^[177] reported a polymer-functionalized rGO to coload curcumin and paclitaxel for highly potent synergistic anticancer treatment. It is well known that although chemotherapy could suppress the cancer development, its adverse side-effects and drug resistance in tumors were major concerns in medical application. By contrast, natural anticancer drugs with lower toxicity and safe availability are gaining increasing interest as alternatives for chemodrugs. Therefore, in this study, a commercially potent anticancer drug, paclitaxel, was codelivered with curcumin, a natural product which possesses anti-inflammatory, antioxidant, and antibacterial properties, to enhance the therapeutic efficacy and at the same time reduce its toxicity. As both drugs were hydrophobic in nature, they were loaded onto GO via π - π interaction to increase their solubility and massive delivery. The *in vitro* cell experiments successfully proved that such creative strategy of dual-delivery of chemodrugs was tumor specific toxicity, as they exerted potent killing effect on tumor cell with no significant toxicity on normal cells. Besides, their high toxicity was also confirmed by increased ROS generation, mitochondrial membrane potential depletion, and cell apoptosis results.

The codelivery of cytotoxic agents to specific protease that can response to the malfunctional enzymes in tumor cells has shown promises in practical cancer therapy.^[180] As a representative example, Gu and co-workers designed a furin-mediated sequential delivery of anticancer cytokine and drugs shuttled using graphene as nanocarriers.^[130] To this end, PEG was incorporated to this system to link a furin-cleavable peptide onto GO nanosheets. DOX was then loaded on GO surface by π - π stacking. Finally, tumor necrosis factor (TNF)-related apoptosis-inducing ligand (TRAIL), a typical membrane-associated cytokine, was conjugated onto the system which could specifically target to death receptor on tumor cell membrane to activate apoptosis-mediated cell death (Caspase 3 activation). Once located at tumor site, the plasma membrane-located furin would digest the peptide linker, resulting in the release of TRAIL for apoptosis induction. Then, the nanosystems were internalized by the cells, where DOX could release under the acidic environment (Figure 7). Their results indicated that such DOX induced cytotoxicity, combining with the TRAIL induced apoptosis, had an optimal synergistic anti-tumor activity. This research provided a novel strategy based on graphene-based materials for programmed-drug release, which significantly enhanced cancer treatment efficacy.

Apart from dual drug delivery, combined dual-chemotherapy with other kind of therapeutic strategies also attracts researchers' attention. Tran et al.^[179] developed a GO-based carrier to achieve synergistic chemo/phototherapy for cancer treatment. In this study, dual drugs DOX and irinotecan were coloaded onto the surface of GO for higher cytotoxicity than free single drug. Instead of commonly used DOX, irinotecan, a topoisomerase I inhibitor which could lead to DNA damage and cell death, was codelivered. They also applied NIR irradiation to realize PTT treatment of cancer as well as enhanced drug release. Once exposed to this nanocomposite, more significant morphological changes of cell nucleus and

severe apoptosis were discovered, especially in MDA-MB-231 resistant breast cancer cells. It was discovered that such dual-chemotherapy and PTT could induce cell apoptosis through upregulating p53, p27, and p21 proteins expressions. This study provided a powerful tool for combined dual-chemo-PTT to overcome drug resistance as well as achieve better therapeutic efficacy. More recently, Su et al.^[162] reported another tumor targeted chemo-photothermal therapy based on ultrasmall lipographene nanosponges (Figure 8). Lactoferrin (Lf), which contains targeting and transcytosis modalities, was conjugated to lipid bilayer for enhanced penetration and accumulation in deep tumors. In addition to anticancer drug docetaxel, an energy giver gasified perfluorohexane (PFH) was also delivered onto this nanosponges. Upon NIR irradiation, not only PTT could be triggered, the increased local temperature could also activate the gasification of PFH and consequently cause damage to tumor spheroids. Both *in vitro* and *in vivo* experiments showed that such synergistic effect of gasification and chemotherapy/PTT could significantly suppress tumor with no recurrence.

3.4. Platforms for Combination of Gene Therapy with Chemotherapy

In order to overcome the intrinsic/acquired drug resistance and the drug-dosage limitation, dual delivery chemodrugs with genes have been propounded. Some tumor-specific proteins that alter normal therapeutic pathways of cytotoxic drugs are overexpressed in drug-resistant cancer cells.^[181] GT involves the delivery of genetic materials such as small interfering RNA (siRNA) molecules to express proapoptotic proteins or down-regulate or silence such overexpressed oncogenic proteins to cure or prevent diseases.^[49,182,183] Due to their inert nature, low toxicity and capability of efficiently immobilizing nucleic acid and encapsulating small molecule drugs, graphene-based materials are also widely used for combined chemotherapy and GT.^[184–187]

The commonly used mechanisms of combined GT and chemotherapy are to interfere drug resistance pathway by GT. As a typical example, Zhi et al. synthesized a GO codelivered adriamycin (ADR) and miRNA-21 gene silencing agent to overcome tumor multidrug resistance (MDR) *in vitro*.^[186] The development and progression of MDR is considered to be closely associated with miRNA21 overexpression, therefore by incorporating anti-miRNA21 (siRNA) into the system to inhibit the expression of miRNA21, anticancer drug could be massively accumulated in drug-resistant tumor cells. Their cell experiments also confirmed that the newly prepared codelivering system could lead to enhanced accumulation of ADR in MCF-7/ADR cells (an ADR resistant cell line) and demonstrated much higher cytotoxicity than free ADR. Similar system was also reported by Zhang et al.^[184] via codelivering chemodrug DOX with Bcl-2 targeted siRNA, which can inhibit Bcl-2 expression for enhanced apoptosis in tumor cells, and by He et al.^[188] codelivering chemodrug DOX with short hairpin (sh) ABCG2 RNA to improve the sensitivity of cancer cells to drugs.

In addition to direct gene silencing strategy, delivery of miRNA to upregulate the expression of tumor-suppressed gene

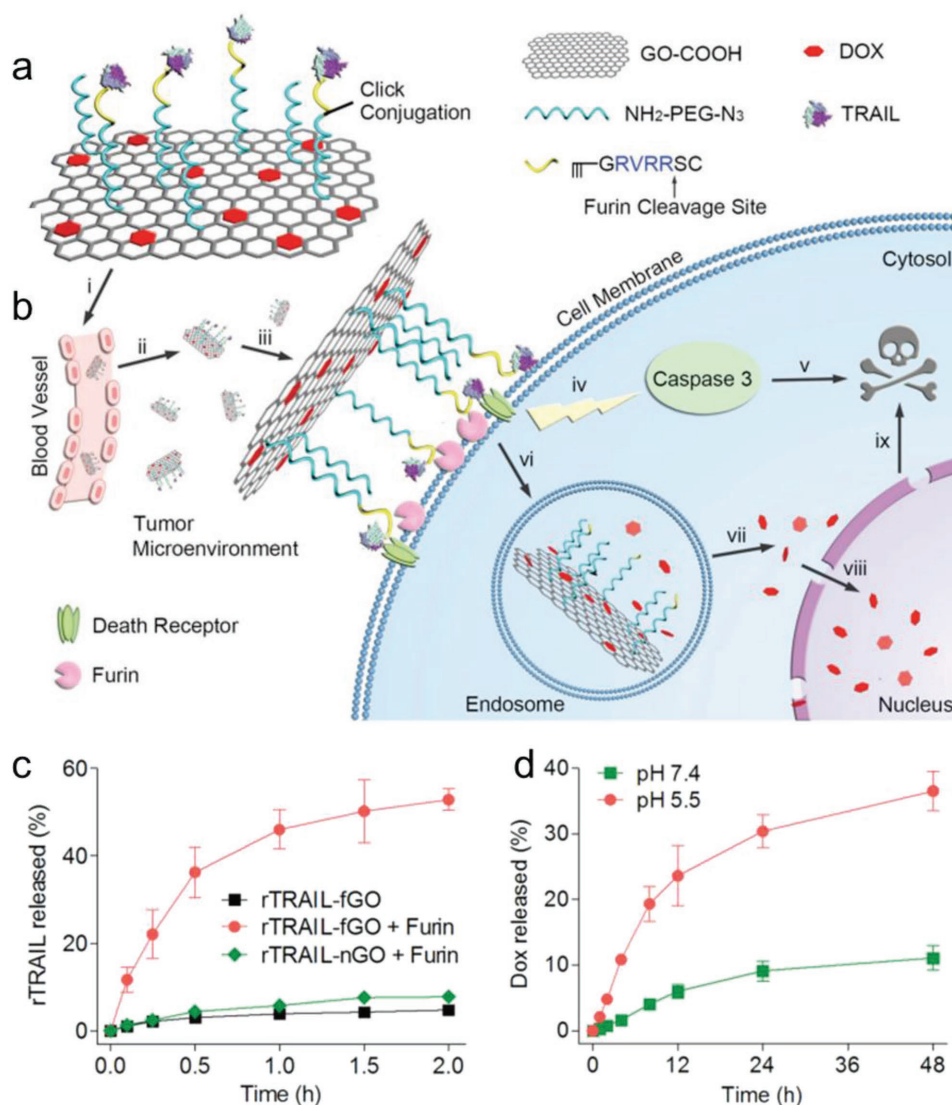


Figure 7. a,b) Schematic design of the cellular protease-mediated graphene-based codelivery system. a) Main components of TRAIL/DOX-fGO, consisting of DOX-loaded GO, PEG linker, and TRAIL-conjugated furin-cleavable peptide. b) Site-specific delivery of TRAIL to cell membrane and DOX to nuclei for enhanced synergistic cancer treatment. i: intravenous administration of GO; ii: accumulation of GO at the tumor site through passive and active targeting effects; iii: TRAIL binding on the death receptor and degradation of peptide linker by furin on the cell membrane; iv: activation of caspase-mediated apoptosis; v: induction of cell death; vi: endocytosis of GO by the tumor cells; vii: acid-promoted DOX release in endosome; viii: accumulation of released DOX into nucleus; ix: induction of DNA damage-mediated apoptosis and cytotoxicity. c) In vitro release profiles of rTRAIL from rTRAIL-fGO or rTRAIL-nGO in the absence and presence of furin. d) In vitro release profiles of DOX from rTRAIL/DOX-fGO at pH 7.4 and 5.5. a–c) Reproduced with permission.^[130] Copyright 2014, Wiley-VCH.

and at the same time inhibit the overexpressed gene is another widely used therapeutic method. For example, Yang et al.^[187] designed a gadolinium-functionalized GO for combined chemotherapy and GT with enhanced therapeutic effects. As reported, downregulation of Let-7 has been observed in many cancers such as lung cancer or melanoma while overexpression of Let-7 has been shown to suppress cancer cell growth. By contrast, Ras proteins such as K-Ras and H-Ras were overexpressed in cancer cells. Consequently, in this study, the authors incorporated the tumor suppressor Let-7 g miRNA into the system with chemodrug epirubicin (EPI) for synergistic chemotherapy/GT. Once the nanocomposites entered tumor cells,

EPI could destroy DNA and Let-7 g miRNA could decrease expression of Ras family proteins to inhibit cell proliferation and reduce tumor growth, thus leading to tumor cell death. In addition, with the good magnetic properties, gadolinium incorporated in this system could be used as excellent MRI contrast agent, providing useful information of nanocomposite accumulation area and concentration of therapeutics within the tumor.

More recently, Zeng et al.^[189] reported another GO-based nanocarriers for codelivering anticancer drug (DOX) with siRNA to inhibit the expression of efflux transporters (P-glycoprotein, P-gp) to defeat drug resistant tumor (Figure 9). DOX and siRNA were loaded onto the nanocarriers by π - π

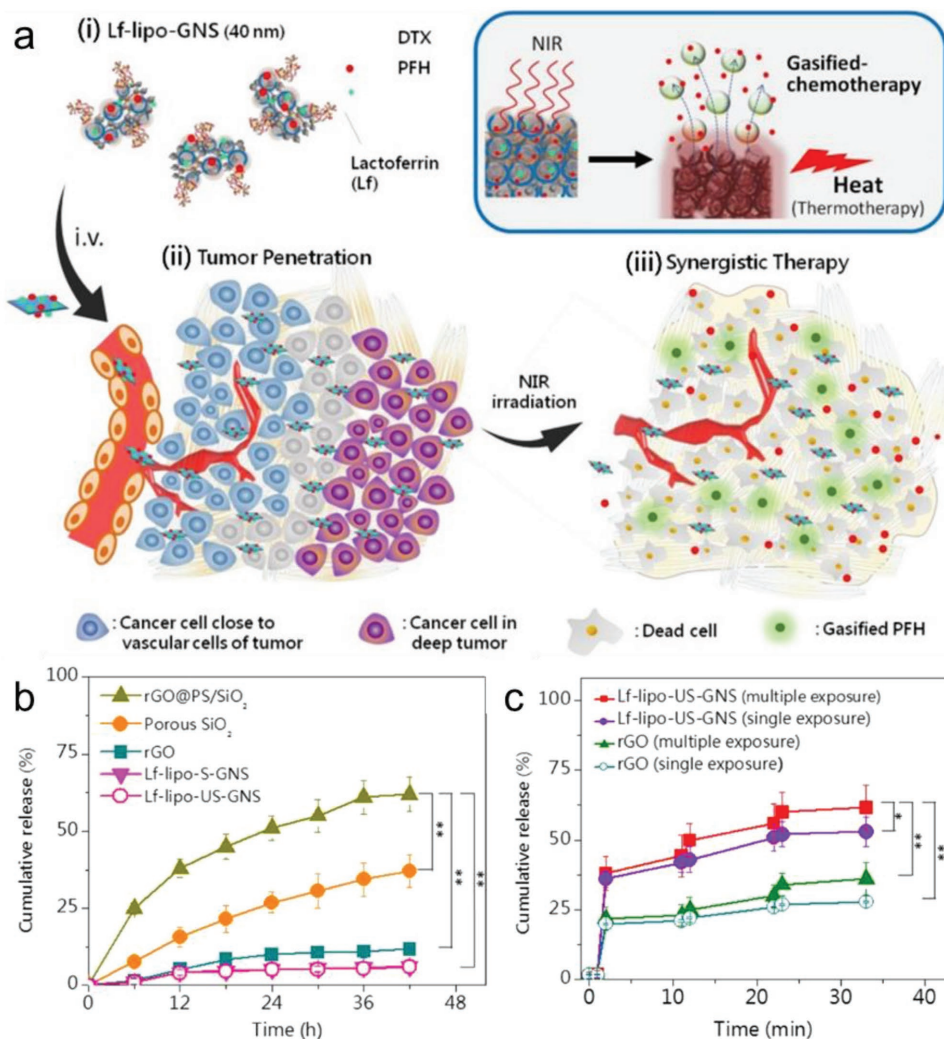


Figure 8. a) Schematic representation of ultrasmall nanosponge-mediated tumor penetration and drug/energy delivery. (i) The protein/lipidcapped graphene nanosponges (40 nm) deliver both DTX and PFH. (ii) Through fluidic protein/lipid-mediated targeting and transcytosis, the nanosponges accumulate in and penetrate tumors. (iii) After NIR irradiation, the intense heat can gasify PFH and release DTX to rupture and eradicate tumor spheroids. b) Drug (DTX) release profiles of rGO, porous SiO₂, rGO@PS/SiO₂, Lf-lipo-S-GNS, and Lf-lipo-US-GNS ($n = 5$, mean \pm s.d., $**p < 0.01$). c) NIR-irradiated DTX release from rGO and Lf-lipo-GNS: single and multiple NIR irradiations (1 min) repeated 3 times after a 10 min waiting time following previous exposure ($n = 4$, mean \pm s.d., $*p < 0.05$, $**p < 0.01$). a–c) Reproduced with permission.^[162] Copyright 2016, American Chemical Society.

stacking and electrostatic interaction, respectively, which could be released in a pH-dependent manner. The silencing of P-gp expression could effectively prevent drug efflux of various hydrophobic anticancer drugs from tumor cells. Upon that, they further incorporated FA into this system to realize a tumor-targeted delivery for efficient chemotherapy and GT. Due to the intrinsic high NIR absorbance of GO, the as-prepared system could be applied for PTT, and hyperthermia could further accelerate the drug release from the nanocarriers. Their in vitro cell experiments indicated that the as-prepared nanosystem could efficiently kill drug-resistant tumor under NIR light irradiation, suggesting successful introduction of a pH-triggered and NIR-triggered and FA receptor targeted gene/drug delivery for synergistic chemo/gene/PTT with improved therapeutic efficacy of drug-resistant tumors.

3.5. Platforms for Combination of Magnetic Hyperthermia Therapy with Chemotherapy

The utilization of combining graphene with magnetic nanoparticles has greatly enriched the biomedical applications of graphene-based material. Iron oxide nanoparticles (IONPs) with excellent magnetic properties are widely used to integrate with graphene-based materials for MRI and MHT or magnetic controlled drug release.^[190] MHT, different from conventional PTT which employs high power laser to generate heat, utilizes magnetic nanoparticles to induce heat by an external alternating current magnetic field. Heat can be generated owing to hysteresis loss or relaxation behavior and it can target deep cancer cells inside the biological system without causing damage to adjacent normal tissue.^[191] Magnetic hyperthermia functions

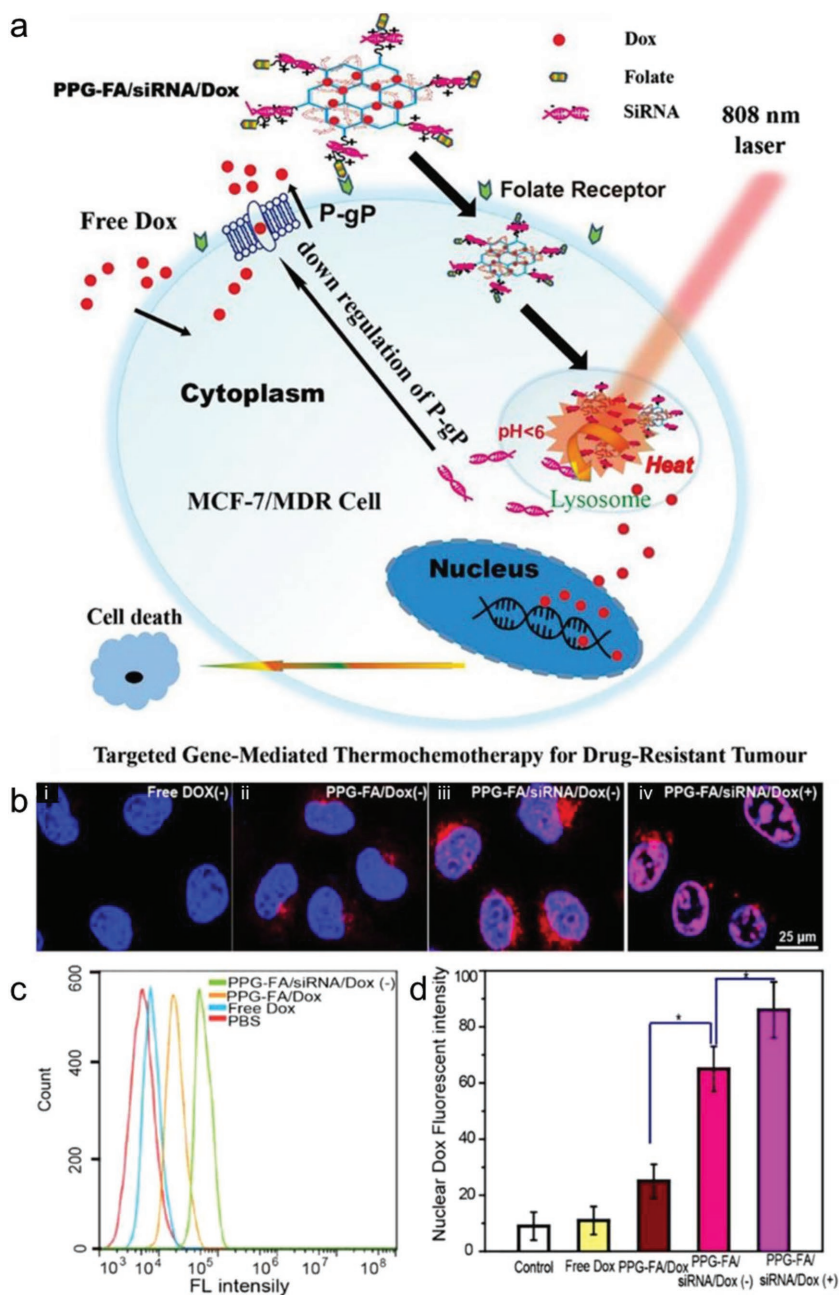


Figure 9. a) Targeted gene-mediated thermochemotherapy for drug-resistant tumour. b) Confocal laser scanning microscope images of MCF-7/ADR cells treated with Dox, PPG-FA/Dox, PPG-FA/siRNA/Dox, and PPG-FA/siRNA/Dox with irradiation. c) Cell uptake of PBS, Dox, PPG-FA/Dox, and PPG-FA/siRNA/Dox for 24 h was measured by flow cytometry. d) The fluorescence signal in MCF-7/ADR nuclei was quantificationally analyzed by Image J software. *P* values in (d) were calculated by Tukey's post-test (**P* < 0.05). a–d) Reproduced with permission.^[189] Copyright 2017, Springer Nature.

to cause protein denaturation, apoptosis, DNA damage, cell growth inhibition, and signaling interruption to cause tumor death.^[39] As magnetic nanoparticles tend to agglomerate in biological vessels, graphene-based materials can serve as a support material to anchor magnetic nanoparticles and improve their

physiological stability. Most importantly, the combining graphene-based materials and magnetic nanoparticles can realize the simultaneous imaging and therapeutic function into one system.

Graphene-based materials in combination with IONPs are widely used in magnetic-guided drug accumulation at the desired tumor site. For example, Yang et al.^[192] synthesized a superparamagnetic GO/Fe₃O₄ hybrid loaded with DOX, where they found that this drug carrier could move regularly in the magnetic field and congregate under acidic conditions such as tumor site. Similarly, Shi and co-workers constructed a multifunctional stimuli-responsive nanosystem cointegrated with super-paramagnetic Fe₃O₄ and paramagnetic MnO_x nanoparticles onto the surface of GO nanosheets.^[54] This nanocomposite could serve as both T₁ and T₂ weighted MRI contrast agents and GO enhanced MHT to tumor targeted imaging and treatment. Besides, they also found that the as-prepared nanocomplex could down-regulate the expression of metastasis related proteins (MMP2, Snail, uPA, etc.) to inhibit the metastasis of cancer cells. Together with massive anticancer drug loaded onto the platform, this nanocomposite could significantly reverse the multidrug resistance of cancer cells. In 2016, Sasikala et al. reported remotely controlled GO nanoheaters for magnetic-induced thermo-chemosensitization.^[193] In their study, GO was conjugated with iron oxide and DOX (GO-IO-DOX) for synergistic MHT and chemotherapy. This novel nanocomposite could deliver heat when an alternating magnetic field is applied and release drug in a pH-dependent manner in cancer environment. Such pH-responsive drug release is also utilized in other studies. More recently, Yao et al.^[194] synthesized graphene quantum dots (GQDs)-capped Fe₃O₄/SiO₂ magnetic mesoporous nanoparticles as a multifunctional platform for controlled drug delivery, MHT and PTT (Figure 10). As demonstrated, controlled drug release could be activated in the acidic environment owing to the pH-dependence of the interaction between mesoporous SiO₂/GQD and drugs. Besides, GQDs in the system with strong NIR absorbance and high photothermal conversion efficiency were utilized for PTT. In addition, Fe₃O₄ nanoparticles

were used to generate heat under alternating magnetic field for hyperthermia therapy. Such hyperthermia could reversely accelerate the drug release. The in vitro experiments successfully showed that the combined chemotherapy, MHT, and PTT exhibited higher efficacy to kill tumor cells compared with any

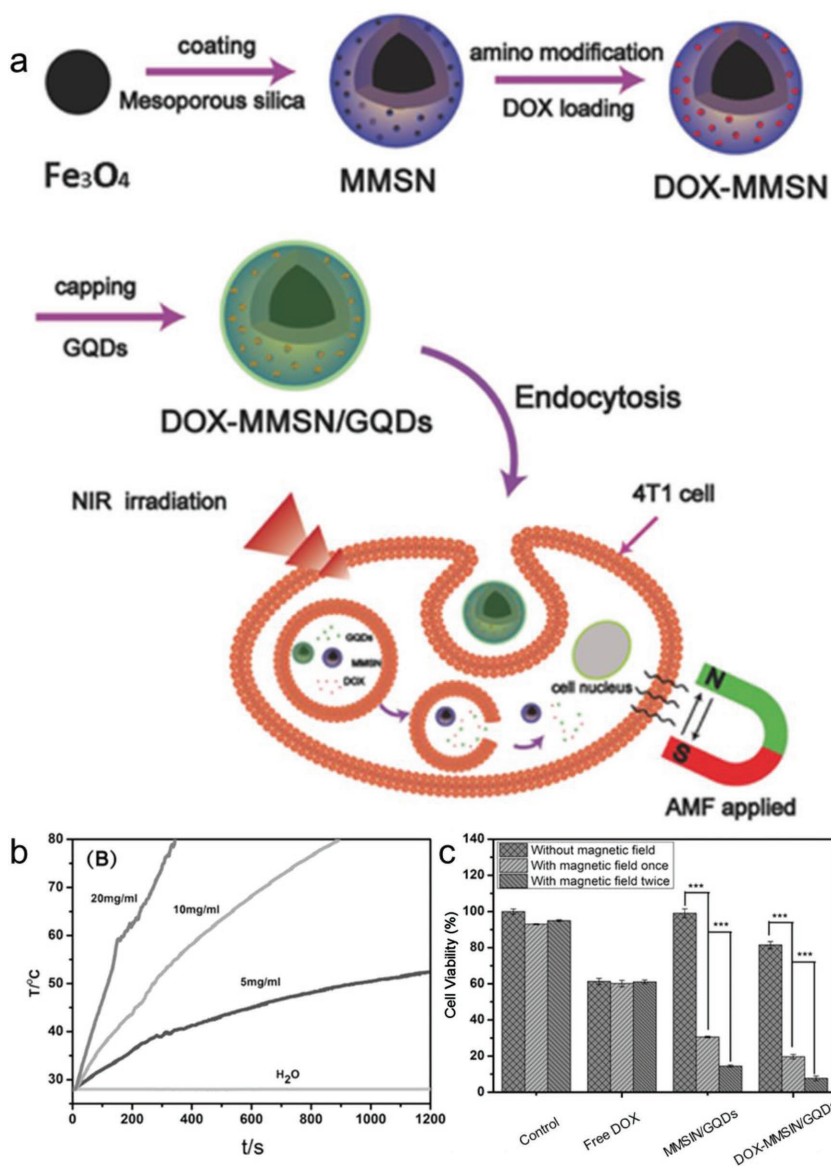


Figure 10. a) Schematic illustration of the preparation process of the DOX-MMSN/GQDs nanoparticles and synergistic therapy combined with controlled drug release, magnetic hyperthermia, and photothermal therapy. b) The magnetic heating curves of the H₂O and MMSN/GQDs suspensions with different concentrations evaluated under an alternating magnetic field with a magnetic field strength of 180 Gauss and a frequency of 409 kHz. c) Cell viability of the 4T1 cells after 8 h incubation with free DOX, MMSN/GQDs, and DOX-MMSN/GQDs suspensions (DOX: 4.7 μg mL⁻¹, MMSN/GQDs: 100 μg mL⁻¹) without and with magnetic field treatment once and twice, and then culture in fresh DMEM culture medium for another 2 h. a–c) Reproduced with permission.^[194] Copyright 2016, Wiley-VCH.

single treatment alone. Moreover, Wo et al.^[195] combined PDT with chemothermal, photothermal, and magnetomechanical therapy into one system for a much more lethal cancer destruction. In this nanocomposite, hollow magnetic nanospheres of Fe₃O₄ were coated with silica shells and conjugated with GQD as a core-shell composite. They further modified the composite with liposome and loaded DOX. Fe₃O₄ nanospheres were used for both magnetic mechanical and PTT application, while GQDs functioned as an excellent photothermal enhancer

due to their good photothermal conversion. Both SiO₂ and GQD could be responsible for ROS generation under laser irradiation. In the end, with massive loading capability, DOX served well for efficient chemotherapy. These successfully proved that the quadruple synergistic effects of magnetomechanical, photothermal, photodynamic, and chemotherapy based on the as-prepared nanoparticles exhibited strongest effect in tumor killing with magnetic field stimulation and NIR laser irradiation.

4. Smart Platforms for Photothermal Therapy-Based Combined Therapy

Apart from their potentials in drug delivery, another unique advantage of graphene-based materials is their good NIR absorption ability and photothermal conversion efficiency, which can be utilized for PTT application. PTT can not only kill the cancer cells that are not sensitive to chemotherapy or RT, but also enhance intratumoral blood flow to improve oxygen status in tumors,^[196] which can synergistically improve the therapeutic effects of various treatments, such as PDT, RT, and chemotherapy. Moreover, the photothermally induced endosomal disruption can also cause drug/gene escape from endosomes and release drug/gene at cytosol for more efficient therapeutic effects.^[197] In this part, we put our focus on the development of smart graphene-based platforms for PTT-based synergistic therapy (Figure 11).

4.1. Platforms for Combination of Photodynamic Therapy with Photothermal Therapy

As mentioned above, PDT is a noninvasive treatment which involves the activation of photosensitizers with specific light to generate ROS, and ultimately leads to cell apoptosis or necrosis.^[169,198] In practice, most commonly used photosensitizers are hydrophobic molecules and thus tend to aggregate in physiological solutions.^[199] Therefore, the effective photosensitizer delivery is the key factor to achieve high PDT efficacy. Graphene-based platforms are ideal carriers for loading and delivering various hydrophobic photosensitizer molecules. When loading with photosensitizers, graphene can function as a good quencher to inhibit ROS generation.^[200] However, once the photosensitizers are released from the graphene upon outside stimuli, the ability of ROS generation can be recovered. This feature makes graphene a smart photosensitizer delivery

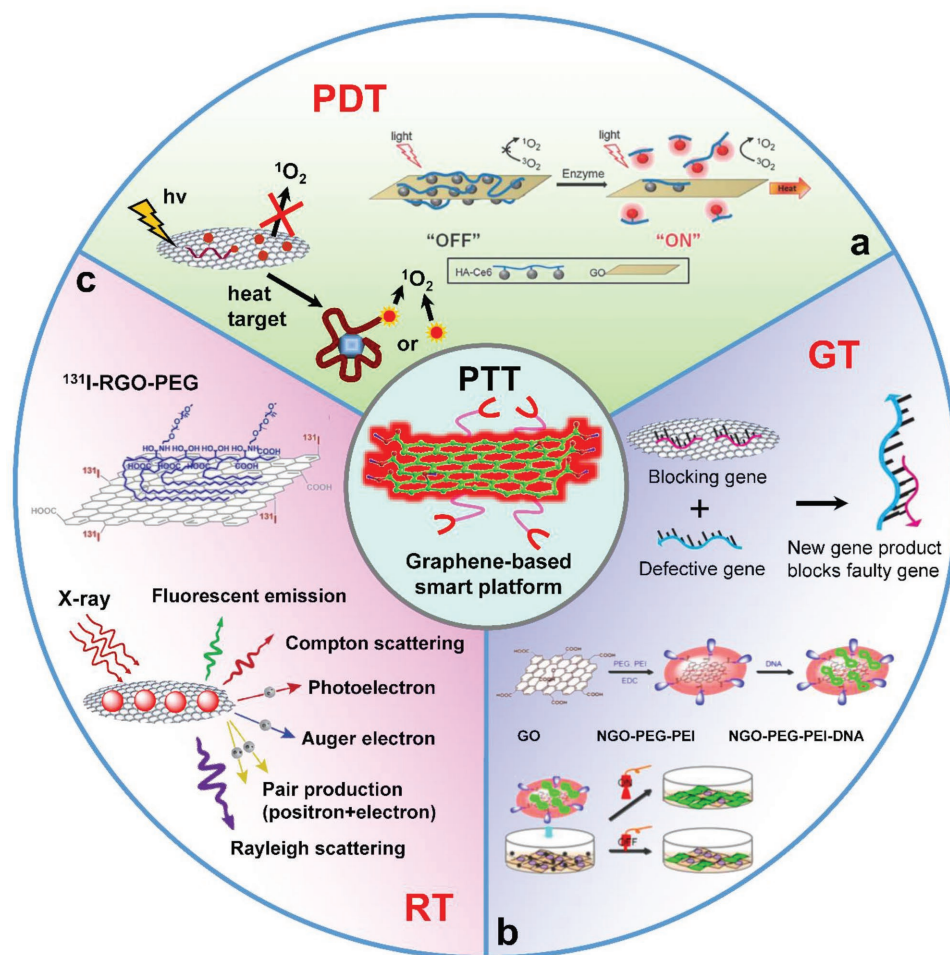


Figure 11. Schematic of graphene-based materials as excellent carriers for PTT-based combined therapy. a) Combination of PDT with PTT. Reproduced with permission.^[117] Copyright 2012, Royal Society of Chemistry. b) Combination of GT with PTT. Reproduced with permission.^[217] Copyright 2013, Wiley-VCH. c) Combination of RT with PTT. Reproduced with permission.^[42] Copyright 2015, Elsevier.

system because graphene-based PDT can be realized in a controlled manner at desirable site. Potential side effects to normal tissue may also be consequently reduced during the delivery process in the body.

The combination of two typical phototherapeutic approaches, PDT and PTT, can realize a superadditive (namely, $1 + 1 > 2$) therapeutic effects.^[201–203] In this combined formulation, mild hyperthermia from PTT is capable of increasing the intracellular photosensitizer concentration via improving the membrane permeability to enhance the tumor cell uptake of photosensitizer-loaded nanocarriers.^[201,204] Besides, mild hyperthermia is also able to accelerate the blood flow to increase the vascular saturated O_2 concentration, which facilitates the elevation of the 1O_2 generation in the oxygen-dependent type II photosensitizers.^[205] Graphene-based materials are reported to be ideal multifunctional platforms for combined PTT–PDT to kill tumor cells.

Tian et al.^[201] for the first time reported that PEG-functionalized GO nanosheets could be used as a simple, but efficient and elegant carriers to load with photosensitizer (Ce6) for photothermally enhanced PDT (PEG–GO–Ce6) (Figure 12). Due to the quenching effect of graphene, the 1O_2 production

ability of Ce6 was significantly inhibited once it was loaded on graphene surface. Following cellular uptake of PEG–GO–Ce6, the generated heat provided by GO nanosheets under NIR light irradiation could cause Ce6 to be released from the surface of GO, resulting in the restoration of 1O_2 production for PDT applications. Moreover, the mild photothermal treatment was able to enhance the intracellular delivery of Ce6 for further improving the PDT efficacy. Later on, Cho and Choi^[165] developed an enzyme-activatable “smart” platform composed of GO nanosheets and photosensitizer (Ce6), which could be used as a biologically tunable theranostic agent for photoinduced cancer therapy. To endow this theranostic agent with the ability of switching “on” and switching “off” its therapeutic functionality, Ce6 was covalently coupled onto the backbone of hyaluronic acid (HA–Ce6), followed by the physical absorption of the as-made conjugates onto the surface of GO, causing efficient quenching of 1O_2 generation. In the presence of hyaluronidase, it was found that Ce6 was released from the surface of GO nanosheets due to the degradation of polymer backbones of the conjugates through preferential cleavage of glycosidic linkages, finally turning on 1O_2 generation. Moreover, the strong photoabsorption of GO could ensure effective NIR-mediated

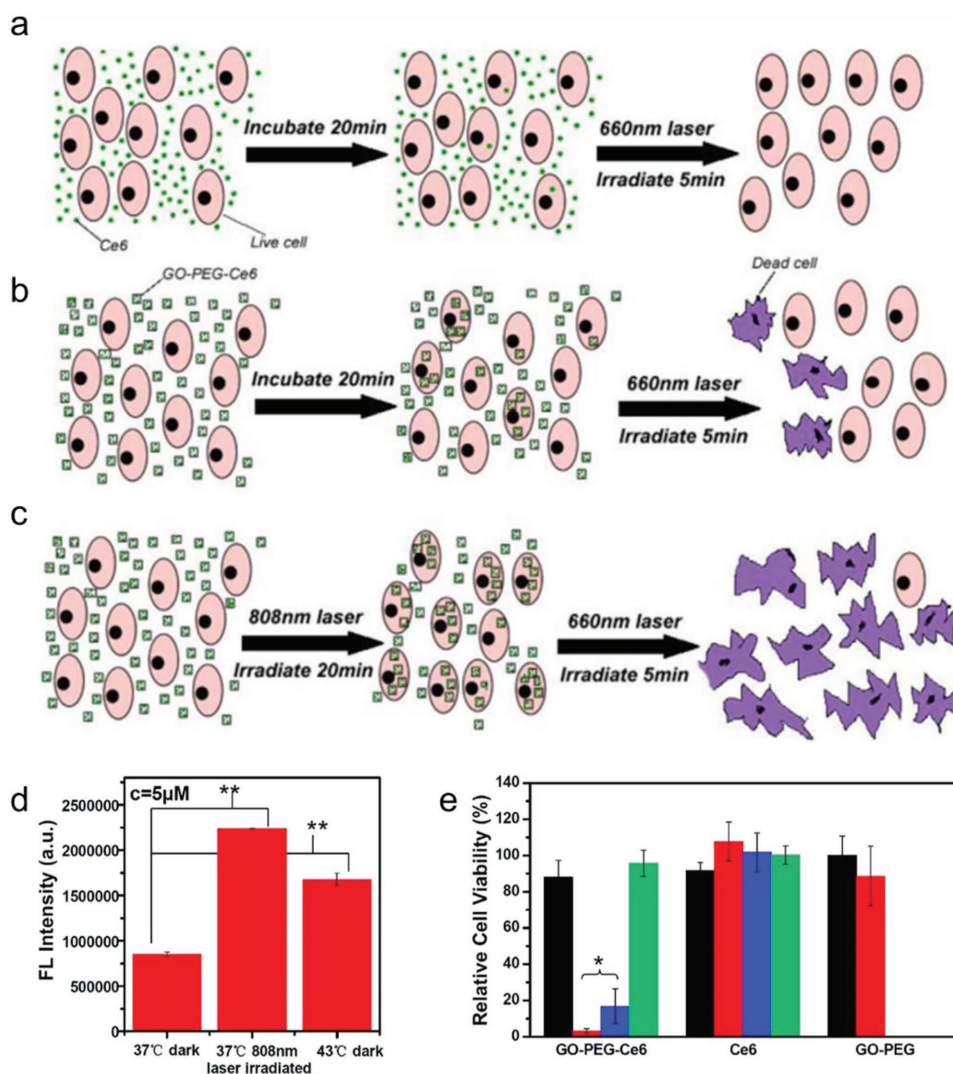


Figure 12. a–c) Schemes of the experimental design in photothermally enhanced photodynamic therapy. KB cells were incubated with a) free Ce6 and b) GO-PEG-Ce6 for 20 min in the dark and then irradiated by the 660 nm laser (50 mW cm^{-2} , 5 min, 15 J cm^{-2}) in control experiments. c) To induce the photothermal effect, GO-PEG-Ce6 incubated cells were exposed to the 808 nm laser (0.3 W cm^{-2} , 20 min, 360 J cm^{-2}) first before PDT treatment. d) Cell uptake of GO-PEG-Ce6 under the three conditions at Ce6 concentrations of $5 \times 10^{-6} \text{ M}$ determined by the measured fluorescence intensities of cell lysate samples. e) Cell viability data of KB cells incubated with GO-PEG-Ce6, free Ce6, or GO-PEG, respectively, at Ce6 concentrations of $5 \times 10^{-6} \text{ M}$. Black, red, blue, and green bars represent samples without any light exposure, with both 808 nm (360 J cm^{-2}) and 660 nm (15 J cm^{-2}) light irradiation, with only 660 nm light exposure, and with only 808 nm light exposure, respectively. Relative cell viabilities in all samples were normalized to the control saline-added samples without laser irradiation (100% viability). Error bars were based on SD of at least four parallel samples. * $p < 0.01$, ** $p < 0.001$. a–e) Reproduced with permission.^[201] Copyright 2011, American Chemical Society.

PTT. Alternatively, Chang et al.^[206] fabricated a biocompatible composite hydrogel composed of rGO, AuNPs, and amaranth extract (AE) for enhanced antitumor therapy by utilizing sequential irradiation as stimuli. Under 808 nm laser irradiation, the precursor solution of rGO, AE, and AuNPs could form a hydrogel shell on cells, which was able to prevent photosensitizer and photothermal agent from migrating to normal tissue. Their results indicated that the $^1\text{O}_2$ produced by AE and the heat generated from rGO and AuNPs could efficiently kill tumor cells with reduced side effects.

To further improve the therapeutic efficiency of graphene-based photosensitizer delivery systems, one strategy is to functionalize graphene and its derivatives with targeting ligands

like HA, endowing them with the ability to target tumor tissues through interactions with tissue-specific receptors.^[126,167,207] In this regard, Huang et al.^[208] reported the fabrication of a targeting photosensitizer delivery system in which GO nanosheets were covalently linked with FA molecules, followed by absorption of Ce6 with the loading efficiency up to $\approx 80\%$. Their results suggested that Ce6 was significantly accumulated within MGC80 cells, causing a remarkable photodynamic efficiency upon irradiation. Moreover, Zeng et al.^[167] developed the FA conjugated polyethylenimine-modified PEGylated graphene loaded with Ce6 (FA-PPG-Ce6). Through the assessment of the cellular uptake and the cellular internalization, it was found that FA-PPG-Ce6 exhibited excellent targeted delivery of Ce6

into the tumor cells to achieve targeted photodynamic killing of cancer cells, while simultaneously showing no obvious toxicity. A novel HA–GO conjugate system was also reported to have the switchable photoactivity of Ce6 (HA–GO/Ce6).^[117] When incubation with HeLa cells which overexpressed HA receptors, the cellular uptake of HA–GO/Ce6 could be effectively improved compared with free Ce6 and the loaded Ce6 molecules were quickly released from HA–GO/Ce6 to recover the photoactivity, finally showing approximately tenfold photodynamic efficiency than that of free Ce6.

4.2. Platforms for Combination of Gene Therapy with Photothermal Therapy

The combination of PTT with GT is another widely studied combined therapeutic strategy.^[209,210] As for GT, the key factor is to develop an efficient gene vector that is capable of protecting oligonucleotides from enzymatic degradation, facilitating cellular uptake with high transfection efficiency, and releasing oligonucleotides from vectors in a sustained and controllable manner. Till now, many gene delivery systems like virions and carbon nanotubes have been developed with high transfection efficiency.^[211,212] The graphene-based materials with large surface area and biocompatibility also render them to be an efficient and safe gene vectors for treatment of cancer cells.^[184,213,214] Once combined with PTT, the hyperthermia induced by graphene and its derivatives can lead to more efficient gene delivery via photothermal-enhanced cellular uptake. Moreover, the generated heat could trigger transient disruption of endo/lysosomal membranes to facilitate the endosomal escape of vectors and then accelerate the release of oligonucleotides from vectors. In turn, GT can cooperatively improve the PTT efficacy via specific inhibition of heat shock protein expression or reduction of the resistance of cancer cells against heat damage.^[39,215] Therefore, the combination of GT and PTT may produce strong synergistic therapeutic effects.

H. Kim and W. J. Kim^[216] fabricated a photothermally controlled gene delivery system via linking branched polyethyl- enimine (BPEI) with rGO using hydrophilic PEG as a spacer (PEG–BPEI–rGO). From the *in vitro* gene transfection study, it was found that PEG–BPEI–rGO exhibited higher gene transfection efficiency than that of unmodified control in National Institutes of Health/3T3 (NIH/3T3) cells and PC-3. Moreover, under NIR laser irradiation, PEG–BPEI–rGO showed higher gene transfection efficiency than that of group without NIR laser irradiation, which was mainly due to the local heat-induced-acceleration of endosomal escape. Another study reported by Yin et al.^[183] showed that GO could be regarded as a gene delivery platform to efficiently codeliver histone deacetylase 1 (HDAC1) and K-Ras siRNAs to specifically target pancreatic cancer cells. Moreover, under NIR light irradiation, they found that the synergistic combination of GT and PTT exhibited significant anticancer efficacy, inhibiting *in vivo* tumor volume growth more than 80% (Figure 13). Feng et al. also demonstrated the PEG/PEI-modified nano-GO conjugate (NGO–PEG–PEI) as the light-responsive gene carrier which showed superior gene transfection efficiency without serum interference or reduced cytotoxicity compared to free PEI or GO–PEI conjugate.^[217] Moreover, they further found

that the mild hyperthermia could result in the enhancement of the cellular uptake of NGO–PEG–PEI due to the increased cell membrane permeability. These study encourages further explorations of functionalized GO nanosheets as a photocontrollable nanovector for the combination of PTT and GT.

4.3. Platforms for Combination of Immunotherapy with Photothermal Therapy

It is reported that some graphene-based materials can directly stimulate immune effects through the interaction with the cellular pathogen sensors in immune cells.^[218–220] For example, the work of Donaldson and co-workers showed that the accumulation of graphene nanoplatelets could cause excessive inflammatory responses, including both macrophages and granulocytes.^[221] Chen et al. reported that GO itself can induce toll-like receptors (TLR) responses (triggering TLR-4 and TLR-9 signaling cascades) and autophagy in tumor cells and thus inhibit tumor growth *in vivo*.^[222] In addition, as a good delivery platform, graphene based materials are also used as delivery systems in immunotherapy.^[223–225] For instance, in 2017, Yu et al. developed a tumor integrin $\alpha\beta6$ -targeting peptide-functionalized GO loading with photosensitizers.^[225] They found that the newly synthesized nanocomposites could remarkably prevent tumor growth by improving the infiltration of cytotoxic CD8⁺ T lymphocytes inside tumors. With the targeting peptide, this tumor-targeted PDT could effectively ablate tumors with immunological memory. Lately, the combination of the intrinsic PTT ability of graphene-based materials with immunotherapy is also attracting much attentions.^[226] As a representative example, Qu and co-workers reported an immunostimulatory oligonucleotides-loaded cationic GO for combined PTT/immune cancer therapy.^[227] In this study, cytosine-phosphate-guanine (CpG) was used as an immune system trigger, as it can be recognized by mammalian immune system through TLR9 and consequently cause proinflammatory cytokines (including TNF- α and IL-6) secretion.^[228] The dual-polymer (PEG and PEI) functionalized GO was served as an efficient CpG oligonucleotides transporter into target tumor cells without intracellular degradation. As their results go, the application of NIR irradiation could significantly enhance the immunostimulation responses, possibly because the photo-induced hyperthermia could accelerate intracellular trafficking of nanovectors. Their work successfully provided a safe and efficient nanocomposite for enhanced immune-stimulation and synergistic photothermal/immune cancer therapy.

4.4. Platforms for Combination of Radiotherapy with Photothermal Therapy

The oxygen-deficient tumor microenvironment has been evidenced to be capable of decreasing the sensitivity of cancer cells to X-ray/ γ -ray irradiation, thus rendering RT ineffective in the treatment of hypoxic solid tumors.^[39,229] To overcome this issue, PTT may be implemented before RT because hyperthermia acts as a physical alternative to improve tumor oxygenation via increasing the intratumoral blood flow.^[230–232]

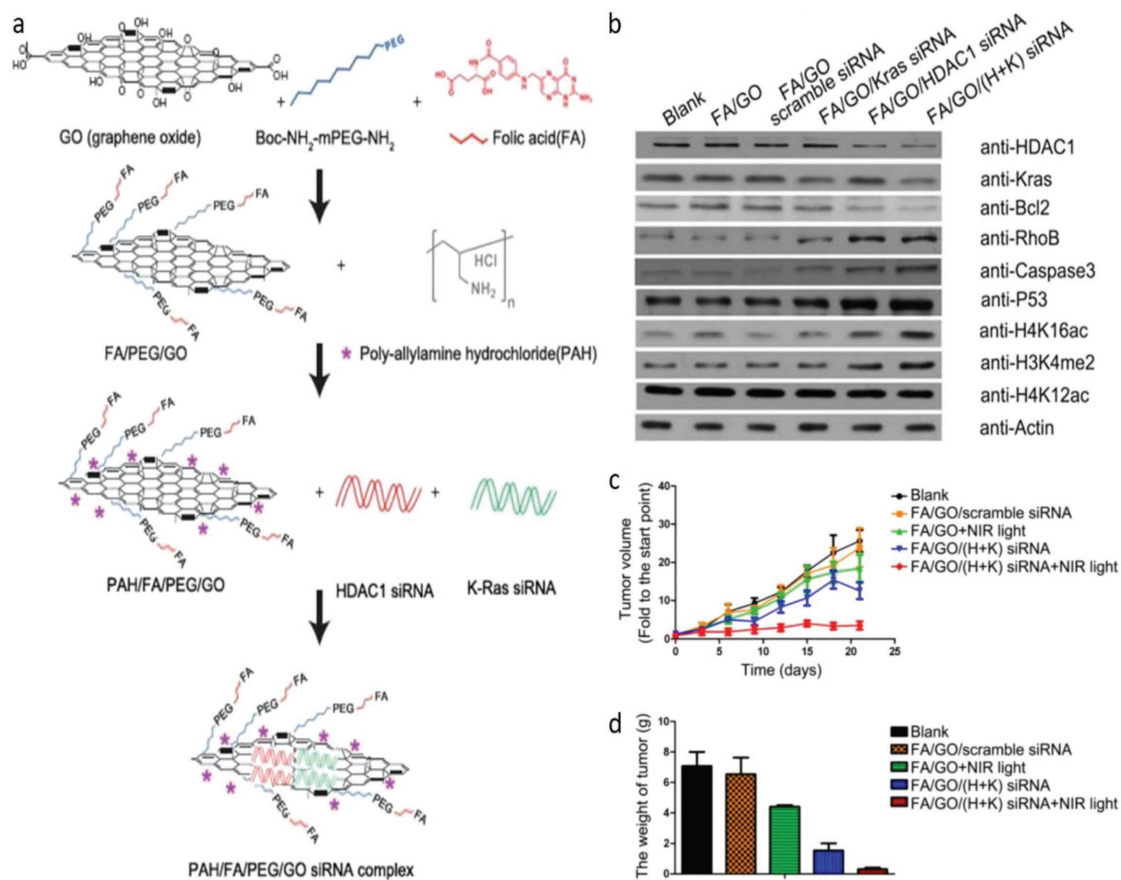


Figure 13. a) Schematic overview of the FA/PEG/GO synthesis and gene loading process using engineered GO-based nanocarriers. Folic acid (FA) was conjugated with NH₂-mPEG-NH₂ to form FA/PEG-NH₂. Subsequently, FA/GO nanosheets were prepared by conjugating the amine-functionalized FA/PEG-NH₂ to increase water solubility and biocompatibility. For siRNA delivery, PEGylated or FA/PEGylated GO were functionalized with positive polymer PAH to form positively charged GO/PEG/PAH or GO/PEG/FA/PAH, which were able to deliver siRNA by electrostatic interaction. b) Target gene expression in MIA PaCa-2 cells treated with different nanoformulations. Relative protein levels as detected by western blotting. Actin was used as the protein loading control. Data are presented as means \pm SEM of triplicate experiments. $**P < 0.01$ vs PBS (blank). c,d) Antitumor activities of GO-based nanoformulations in a MIA PaCa-2 xenograft animal model. c) Relative changes in tumor volume over time and d) tumor weights of mice treated with different nanoformulations. Relative tumor volume was defined as $(V - V_0)/V_0$, where V and V_0 indicate the tumor volume on a particular day and day 0, respectively. Error bars represent SEMs for triplicate data. Mean tumor volumes were analyzed using one-way ANOVA. Values represent the means \pm SEM, $n = 4-6$ tumors. a-d) Reproduced with permission.^[183] Copyright 2017, Ivyspring International Publisher.

Together with the fact that hyperthermia can effectively suppress the nonlethal damage repair induced by X-ray radiation, PTT can be combined with RT to establish a light-responsive platform consisting of radioisotope and graphene to give rise to remarkable synergistic PTT/RT effects via the enhancement of PTT on RT. As a representative example, Liu and co-workers^[42] reported a pioneering work that labeled rGO with radionuclide ¹³¹I to form ¹³¹I-rGO and then functionalized with PEG to obtain ¹³¹I-rGO-PEG for combined PTT/RT of metastatic tumors. Most interestingly, the intrinsic higher NIR absorbance and the labeled ¹³¹I-radioactivity could result in the synergistic therapeutic efficacy. As revealed by PET imaging, efficient tumor accumulation of ¹³¹I-rGO-PEG was observed after the intravenous injection. Moreover, the combined PTT/RT remarkably inhibited the growth of tumors in the animal tumor model experiments, providing a potential strategy for combined therapy of tumors (Figure 14). Besides, hybridization of GO with the nanoparticles containing heavy Z atoms such as

Au, Bi, W, and Ba may be another strategy for the construction of nanoscale radiosensitizers for enhancing RT by external-X-ray/ γ -ray radiation. These high-Z atoms can absorb more X-rays and deposit the radiation energy locally within tumor cells for an improved dose-amplification effect. Together with the light responsive property, which can improve tumor oxygenation under NIR light irradiation, the enhancement of RT toward hypoxic cancer cells can be achieved with the minimal side effects.

5. Smart Platforms for Ultrasound Therapy-Based Combined Therapy

Ultrasound, a nontoxic mechanical wave commonly used in diagnostic imaging in clinic, can also exert therapeutic effects on tumor eradication. Ultrasound can effectively activate sonosensitizers to produce ROS to kill cancer cells. In comparison

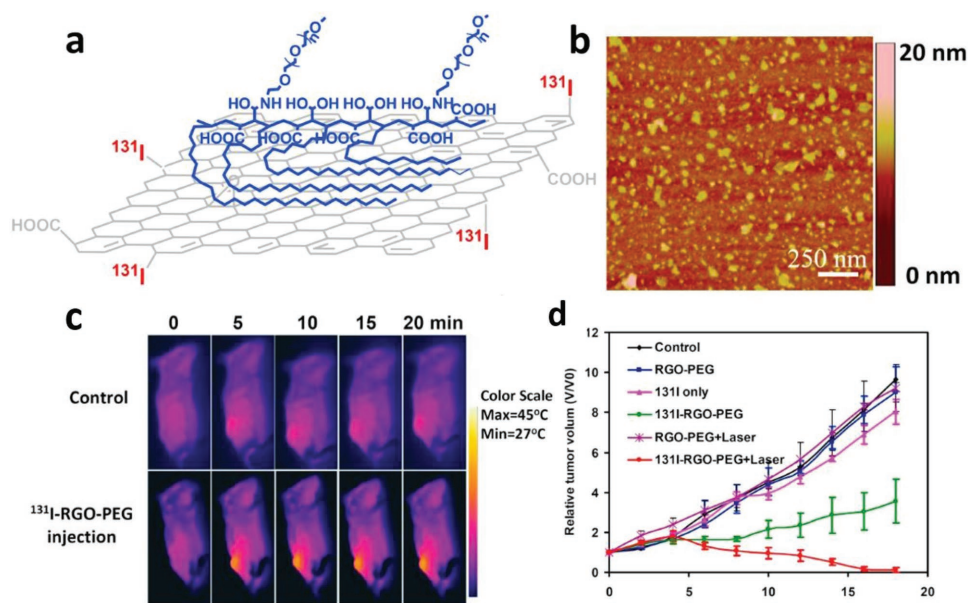


Figure 14. a) A scheme of RGO functionalized with PEG and labeled with ^{131}I . b) An AFM image of RGO-PEG. The size distribution of RGO-PEG was 50–60 nm. c) IR thermal images of tumor-bearing mice exposed to the NIR laser (808 nm, 0.2 W cm^{-2} , 20 min) after i.v. injection with PBS or ^{131}I -RGO-PEG. d) The tumor growth curves of different groups of mice after different treatments indicated. Six groups including untreated mice (control), RGO-PEG injected mice with or without laser irradiation, ^{131}I treated mice (^{131}I only), ^{131}I -RGO-PEG injected mice with or without laser irradiation, were used in this experiment (5 mice for each group). The tumor volumes were normalized to their initial sizes. Error bars were based on standard derivations of 5 mice per group. a–d) Reproduced with permission.^[42] Copyright 2015, Elsevier.

with conventional PDT that utilizes visible light to induce ROS generation, ultrasound is a mechanical wave that can penetrate through biological tissues without depth limitation.^[144] In addition, SDT can focus numerous ultrasound waves on target tumors through fast ultrasound energy deposition to destroy tumor vasculatures and tumor cells with minimal damage to surrounding healthy tissues.^[39] Graphene-based materials, such as graphene, GO, and rGO, are widely used for enhancing SDT outcomes because of their high electroconductivity, large surface-to-volume ratio, and high photothermal-conversion capability.^[26,27,233] For example, Dai et al. demonstrated a graphene augmented sonocatalytic tumor ablation.^[27] It was previously reported that TiO_2 nanoparticles can produce ROS upon ultrasound activation but of relatively low level, which fails to further separate electron and hole pairs from energy band. Therefore, single TiO_2 induced SDT efficiency is relatively low. To solve this problem, the researchers creatively integrated 2D graphene with TiO_2 nanosensitizers for enhanced SDT efficacy. Due to the high electroconductivity, graphene could separate the electrons and holes, and prevent them from recombination upon external ultrasound irradiation. Besides, upon 808 nm laser irradiation, graphene with high photothermal conversion could synergistically improve the SDT effects (Figure 15). Their findings proved that the designed nanocomposites could reach higher tumor-growth-inhibition rate in comparison to single TiO_2 based nanosensitizers.

Apart from SDT, graphene-based materials are also reported to be able to realize an ultrasound hyperthermia to cancer therapy. Compared with traditional NIR-triggered PTT, ultrasound hyperthermia can achieve better therapeutic outcomes,

as ultrasound is a clinically used method with low toxicity and able to realize limitless penetration through tissue. Through the formation of cavitation bubbles and elevated temperature, ultrasound can not only trigger drug release, but also improve the permeability of biological barriers (such as cell membranes or blood brain barrier) to increase drug diffusion.^[122] In 2013, Yang et al.^[233] synthesized a smart magnetic GO based nanocomposite to realize a noninvasive combined treatment of brain tumors through targeted chemotherapy and amplified ultrasound-hyperthermia therapy. The nanosystem could carry toxic drug epirubicin and accurately deliver it to tumor site with super high drug concentration (14.7-fold higher than surrounding tissues) upon external magnetic stimulus. Besides, the highly concentrated GO could also serve as a heat-conducting base to increase local temperature upon application of focused-ultrasound. This synergistic chemotherapy/SHT system showed profoundly improved antitumor efficacy for gliomas. Moreover, such ultrasound hyperthermia could also cofunction with SDT for tumor ablation. Chen et al. reported a delicate theranostic rGO@mesoporous silica-iron oxide nanoparticle-Rose Bengal (rGO@MSN-IONP-RB) nanocarrier for SDT and ultrasound hyperthermia for combined cancer treatment.^[26] $^1\text{O}_2$ was generated by ultrasound-activated RB, and rGO was served as a heat-conducting base to elevate local temperature using extremely low-power focused ultrasound irradiation, leading to deep-seated targeted hyperthermia for improving cytotoxic effects in cancer cells. With the magnetic navigation from IONPs, the therapeutic efficacy of the newly synthesized nanocarriers could be largely enhanced due to the precisely targeted accumulation at tumor site.

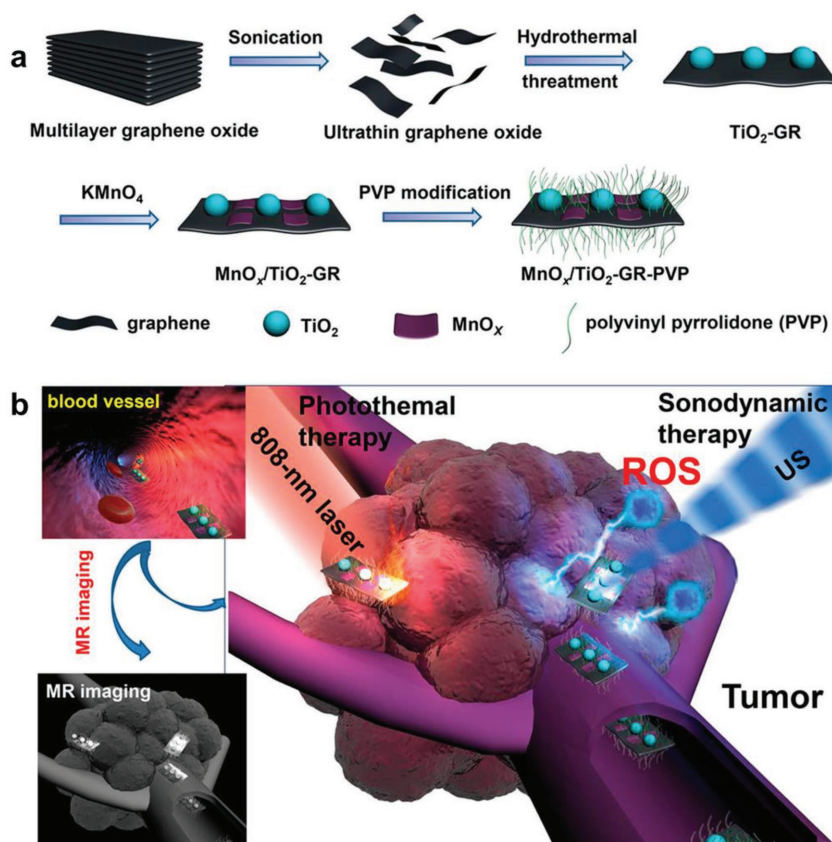


Figure 15. Schematic illustration of the synthetic procedure of $\text{MnO}_x/\text{TiO}_2\text{-GR-PVP}$ and MR imaging-guided synergistic SDT/PTT against cancer. a) Scheme of the synthetic procedure for $\text{MnO}_x/\text{TiO}_2\text{-GR-PVP}$ nanocomposites, including exfoliation of GO, hydrothermal treatment for the integration of GO with TiO_2 , in situ redox reaction between $\text{TiO}_2\text{-GR}$ and postintroduced KMnO_4 , and surface PVP modification. b) Schematic illustration of theranostic functions of $\text{MnO}_x/\text{TiO}_2\text{-GR-PVP}$ nanocomposites, including free transport with the blood vessels after intravenous injection, TME-responsive MRI guidance prior to cancer therapy, and synergistic SDT/PTT against cancer. a,b) Reproduced with permission.^[27] Copyright 2017, American Chemical Society.

6. Outlook and Perspective

Here, we have summarized the recent advances of using graphene-based nanoplatoms for stimuli responsive code-livery of multiple therapeutic agents or coadministration of various treatment modalities to realize synergistic therapeutic outcome (Table 1). Although current advances are remarkable and exciting, only a few nanocomposites have been evaluated in animal model and none of them have been applied in clinic. Thus, more efforts are still required on several unresolved critical issues which greatly hinder the clinical translation of graphene-based therapeutics.

First, a comprehensive evaluation of the safety of these materials is highly desired before being translated into clinical practice. Most recent studies have proved that graphene materials possess good biocompatibility and low toxic profile.^[62] Proper functionalization of graphene-based materials could also obtain enhanced biocompatibility and lower toxic effects. However, the biocompatibility is not the only factor that should be considered before clinical translation. In addition to toxicity study, the

distribution and excretion of graphene based materials is also important in practical use.^[234] It is widely accepted that graphene is initially distributed to different organs but ends up accumulating in the liver and spleen.^[235,236] Even though the enhanced permeability and retention effect may improve their tumor uptake, it is still encouraged to improve the targeting ability of graphene-based materials by altering administration pathway or surface modification. In addition, some of compounds such as inorganic particles are widely integrated with graphene to endow them with novel properties for bioimaging and therapy modalities. However, those inorganic nanoparticles such as Fe_3O_4 and Au are not biodegradable, which cause serious concern about their toxicity issue, since they may accumulate in living organism for a long time. Therefore, the systematic study on their toxic issue and biological behavior in vivo, such as stability, biodistribution, metabolism, excretion, and long-term effects on the body, which is still in its early stages, should be carried out to ensure the safety of these materials for better clinical use. One of the possible solutions is optimizing the composition of the nanoparticles for a more biodegradable way (e.g., from SiO_2 to organosilica) and the other efficient way is to reduce their particle sizes.^[237] The small size of nanoparticles may exhibit easy excretion out of the body through renal pathway, which can potentially overcome their biodegradation difficulties. Besides, graphene based nanocomposites coated with biocompatible moieties that smaller than 100 nm in size are also believed to be able to clear from the body without causing noticeable toxicity after systemic administration.^[238]

Second, due to the introduction of various functional components such as particles, biological molecular, or polymers for multi-functionality, these composites are not easy to be produced in industrial scale. Thus, the complexities and difficulties in manufacturing and assessment clearly limit their further application from bench to bedside. In practical application, the standardized green and easy performance for safe and functional nanoparticles is always desired. It is believed that, the neater, the better.

Third, rationally combining the therapeutic modalities into graphene-based nanoplatom for “smart” drug delivery and combined cancer therapy is still a challenge. Despite some combination formulations have been successfully proposed and demonstrated remarkable therapeutic effects, investigations related to graphene-based combined therapy are still at the early stage and many important issues need to be solved. For example, in consideration of efficient and successful cancer therapy, the designed nanocomposites should possess both diagnostic and therapeutic functionalities in nature. It is only the imaging guidance that can provide us a more accurate structure

Table 1. Overview of graphene-based materials applied in combined cancer therapies. GQD: graphene quantum dots; GO: graphene oxide; rGO: reduced graphene oxide; PTT: photothermal therapy; PDT: photodynamic therapy; GT: gene therapy; MHT: magnetic hyperthermia therapy; RT: radiotherapy; SHT: ultrasound hyperthermia therapy; SDT: sonodynamic therapy; NIR: near-infrared; DOX: doxorubicin; ZIF-8: Zeolitic imidazolate framework-8; PEG: polyethylene glycol; PAH: poly (allylamine hydrochloride); DA: 2,3-dimethylmaleic anhydride; IL-13: interleukin 13; HA: hyaluronic acid; ADH: Adipic acid dihydrazide; MSN: mesoporous silica nanoparticles; Lf: lactoferrin; PVP: polyvinylpyrrolidone; CT: computed tomography; PAT: photoacoustic tomography; Alg: alginate; PEI: polyethylenimine; Ce6: chlorin e6; SN-38: 7-ethyl-10-hydroxycamptothecin; ZnPc: Zn(II)-phthalocyanine; CPT: camptothecin; MTX: methotrexate; TRAIL: tumor necrosis factor-related apoptosis-inducing ligand; DTX: Docetaxel; PFH: Perfluorohexane; ADR: Adriamycin; SPIO: Superparamagnetic iron oxide; EPI: Epirubicin; Aco: aconitic anhydride; AMF: alternating magnetic field; MFG: magnetic and fluorescent graphene; SiNc₄: silicon naphthalocyanine bis (trihexylsilyloxy); LFUS: low-power focused-ultrasound; RB: Rose Benga; CpG: cytosine-phosphate-guanine.

Graphene structures	Cancer type	Active moiety	Stimulus	Therapeutic remarks	Ref.
GQD-ZIF-8-DOX	4T1 cells	DOX, GQD mediated hyperthermia	pH	Chemotherapy + PTT	[154]
GO-PEG/PAH-DA/DOX	MCF-7 and MCF-7/ADR cells	DOX, GO mediated hyperthermia	pH	Chemotherapy + PTT	[100]
Graphene-silica-PEG-(IL-13 peptide)-DOX	Glioma cells	DOX, graphene mediated hyperthermia	pH, NIR	Chemotherapy + PTT, IL-13R α 2 targeted delivery	[152]
GO-Au-HA-AHD-DOX	Huh-7 and CHO cells	DOX, GO/Au mediated hyperthermia	pH, NIR	Chemotherapy + PTT, HA receptor targeted delivery	[159]
rGO@MSN-HA-DOX	HeLa cells	DOX, rGO mediated hyperthermia	pH, NIR	Chemotherapy + PTT, HA receptor targeted delivery	[160]
rGO-Lf-DOX	RG2 and MCR-5 cells	DOX, rGO mediated hyperthermia	pH, NIR	Chemotherapy + PTT; Lf targeted delivery	[161]
rGO/Bi ₂ S ₃ -PVP-DOX	Hela, MCF-7, HepG2 and BEL-7402 cells	DOX, rGO mediated hyperthermia	pH, NIR	Chemotherapy + PTT; dual CT and PAT imaging contrast agent	[156]
GQD-MSN-DOX	4T1 cells	DOX, GQD mediated hyperthermia	pH, NIR	Chemotherapy + PTT	[153]
GO-Alg-DOX	A549 cells	DOX, GO mediated hyperthermia	pH, GSH	Chemotherapy + PTT	[157]
rGO-BPEI-PEG-DOX	PC-3 and Hela cells	DOX, rGO mediated hyperthermia	pH, GSH, NIR	Chemotherapy + PTT	[53]
GO-PEG-DOX/Ce6	SCC7 cells	DOX, Ce6	660 nm LED	Chemotherapy + PDT	[170]
GO-SN-38-hypocrellin A	A549 cells	SN-38, hypocrellin A	470 nm LED	Chemotherapy + PDT	[171]
GQD-Ag-PEG-DOX	HeLa, DU145 cells	DOX, Ag	pH, 425 nm LED	Chemotherapy + PDT	[173]
Graphene-(poly-L-lysine)-DOX-ZnPc	HeLa, MCF-7, B16 cells	DOX, ZnPc	pH, 440 nm light	Chemotherapy + PDT	[172]
rGO-Au-spinach extract-Fluorouracil	Hela, CHO cells	Fluorouracil, spinach extract/Au induced ROS, rGO/Au mediated hyperthermia	pH, 660 nm light	Chemotherapy + PDT + PTT	[174]
rGO-PF-127-Curcumin-Paclitaxel	A549, MDA-MB-231 cells	Curcumin, Paclitaxel	pH	Dual chemotherapy	[177]
GO-Fe ₃ O ₄ -CPT-MTX	HepG2 cells	CPT, MTX	pH	Dual chemotherapy + PTT	[176]
GO-poloxamer 188-DOX-irinotecan	MDA-MB-231 cells	DOX, irinotecan	pH	Dual chemotherapy + PTT	[179]
GO-PEG-DOX-rapamycin	MDA-MB-231, MCF-7, BT474 cells	DOX, rapamycin	pH	Dual chemotherapy + PTT	[178]
GO-PEG-furin cleavable peptide-TRAIL-DOX	A549 cells	DOX, TRAIL	pH	Dual chemotherapy, TRAIL targeted delivery	[130]
Graphene-Lf-DTX-PFH	GR2 tumor	DTX, PFH	NIR	Dual chemotherapy (drug + energy), Lf targeted delivery	[162]
GO-PEI-DOX-siRNA	Hela cells	DOX, Bcl-2-targeted siRNA	N.A.	Chemotherapy + GT	[184]
GO-PEI-PSS-ADR-(anti-miR-21)	MCF-7, MCF-7/ADR cells	ADR, anti-miR-21	N.A.	Chemotherapy + GT	[186]
rGO-chitosan-SPIO-DOX-DNA	A549, C4-2b cells	DOX, DNA	pH	Chemotherapy + GT	[185]
GO-Gd-Poly-amido-amine-EPI-miRNA	glioblastoma (U87) cells	EPI, Let-7 g miRNA	pH	Chemotherapy + GT	[187]
GO-chitosan-Aco-PEG-PEI-DOX-shRNA	HepG2 cells	DOX, shRNA(shABCG2)	pH	Chemotherapy + GT	[188]

Table 1. Continued.

Graphene structures	Cancer type	Active moiety	Stimulus	Therapeutic remarks	Ref.
GO-PEI-folic acid-DOX-siRNA	MCF-7/MDR cell	DOX, siRNA	pH, NIR	Chemotherapy + GT; folate receptor targeted delivery	[189]
GQD/MSN/ Fe ₃ O ₄ -DOX	4T1 cells	DOX, MSN/Fe ₃ O ₄ mediated magnetic hyperthermia; GQD mediated photo-hyperthermia	pH, AMF, NIR	Chemotherapy + MHT + PTT	[194]
GQD-Fe ₃ O ₄ / SiO ₂ -liposome-DOX	Eca-109 cell	DOX, Fe ₃ O ₄ mediated magnetic; Fe ₃ O ₄ /GQD mediated hyperthermia; GQD/SiO ₂ induced ROS	NIR, magnetic field	Chemotherapy + magneto-mechanical + PTT + PDT	[195]
GO-PEG-Ce6	KB cells	Ce6 induced ROS; GO mediated hyperthermia	660 nm and 808 nm light	PTT + PDT	[201]
GO-PEG-Ce6	4T1 cells	Ce6 induced ROS; GO mediated hyperthermia	660 nm and 808 nm light	PTT + PDT	[244]
GO-PEG-folate	B16F0 cells	GO induced ROS and mediated hyperthermia	980 nm light	PTT + PDT	[245]
MFG-SiNc ₄	HeLa cells	SiNc ₄ induced ROS; GO mediated hyperthermia	775 nm light	PTT + PDT	[202]
rGO-ZnO-HA	MDA-MB-231 cells	ZnO induced ROS; rGO mediated hyperthermia	365 nm and 808 nm light	PTT + PDT	[246]
GO-HA-Ce6	A549 cells	Ce6 induced ROS; GO mediated hyperthermia	Hadase, 670 nm and 810 nm light	PTT + PDT, Hadase degrades HA to release Ce6	[117]
UCNPs-NGO/ZnPc	HeLa cells	ZnPc induced ROS; GO mediated hyperthermia	630 nm and 808 nm light	PTT + PDT	[204]
PEG-BPEI-rGO/pDNA	NIH/3T3 cells	GO mediated hyperthermia, pDNA	808 nm light	PTT + GT	[216]
GO/FA/siRNA	MIA PaCa-2 cells	GO mediated hyperthermia, siRNA	808 nm light	PTT + GT	[183]
NGO-PEG-PEI	HeLa cells	GO mediated hyperthermia, siRNA	808 nm light	PTT + GT	[217]
GO-PEG-PEI-CpG	RAW264.7 cells	GO mediated hyperthermia; CpG induced immune response	808 nm light	PTT + Immunotherapy	[227]
¹³¹ I-rGO-PEG	4T1 cells	¹³¹ I mediated RT; rGO mediated hyperthermia	808 nm light and X-ray	PTT + RT	[42]
GO-PEG-EPI	GL261 cells	GO mediated hyperthermia, EPI	LFUS irradiation, pH	SHT + Chemotherapy; magnetic guided targeting	[233]
rGO@ MSN-IONP-PEG-RB	SKBr3 cells	RB induced ROS; rGO/IONP enhanced hyperthermia	FUS irradiation	SDT + SHT	[26]
GO-TiO ₂ -MnOx-PVP	4T1 cells	TiO ₂ induced ROS; GO mediated hyperthermia	NIR, ultrasound	SDT + PTT	[27]

and location information for precise therapy. Additionally, code-livery of two or more drugs at one graphene platform may not ensure the synergistic anticancer efficiency. Such drugs are required to be programmed released to realize their synergistic effects. Moreover, when combing chemotherapy with physical treatments such as PTT and PDT, we should also consider their unique spatiotemporal aspects for targeted cancer treatment. For example, in PDT-chemotherapy combined formulation, PDT can quickly kill cancer cells by generating the considerable amount of ¹O₂ upon laser irradiation, but it usually takes time for chemotherapy to exhibit therapeutic outcomes in clinical applications. Last but not least, as tumors are mostly located inside the body instead of on the surface, it is also desirable to apply deep penetrating treatment strategies, such as X-ray (RT), magnetic field (MHT), or ultrasound waves (SDT). Such novel treatment strategies show better penetrating and therapeutic efficacy compared with ultraviolet induced PDT or NIR irradiated PTT. Overall, the rational design and construction of

graphene-based systems for combination-therapy require comprehensive and strong cooperation of experts from different research fields, ranging from cancer biology, chemistry, nanotechnology, material science, and pharmacy.

Acknowledgements

This work was supported by the National Basic Research Program of China (Grant No. 2016YFA0201600), National Natural Science Foundation of China (Grant Nos. 51772292, 31571015, 11621505, 11435002, and 21320102003), Key Research Program of Frontier Sciences (Grant No. QYZDJ-SSW-SLH022), and Youth Innovation Promotion Association CAS (Grant No. 2013007).

Conflict of Interest

The authors declare no conflict of interest.

Keywords

combined cancer therapy, graphene-based materials, smart platforms, stimuli

Received: January 30, 2018
Revised: March 25, 2018
Published online:

- [1] C. Chung, Y. K. Kim, D. Shin, S. R. Ryoo, B. H. Hong, D. H. Min, *Acc. Chem. Res.* **2013**, *46*, 2211.
- [2] K. Yang, L. Feng, X. Shi, Z. Liu, *Chem. Soc. Rev.* **2013**, *42*, 530.
- [3] S. Goenka, V. Sant, S. Sant, *J. Controlled Release* **2014**, *173*, 75.
- [4] Y. W. Chen, Y. L. Su, S. H. Hu, S. Y. Chen, *Adv. Drug Delivery Rev.* **2016**, *105*, 190.
- [5] R. Geetha Bai, N. Ninan, K. Muthoosamy, S. Manickam, *Prog. Mater. Sci.* **2018**, *91*, 24.
- [6] M. Nurunnabi, K. Parvez, M. Nafujjaman, V. Revuri, H. A. Khan, X. L. Feng, Y. K. Lee, *RSC Adv.* **2015**, *5*, 42141.
- [7] C. McCallion, J. Burthem, K. Rees-Unwin, A. Golovanov, A. Pluen, *Eur. J. Pharm. Biopharm.* **2016**, *104*, 235.
- [8] Z. Liu, J. T. Robinson, X. Sun, H. Dai, *J. Am. Chem. Soc.* **2008**, *130*, 10876.
- [9] X. Sun, Z. Liu, K. Welscher, J. T. Robinson, A. Goodwin, S. Zaric, H. Dai, *Nano Res.* **2008**, *1*, 203.
- [10] S. C. Patel, S. Lee, G. Lalwani, C. Suhrland, S. M. Chowdhury, B. Sitharaman, *Ther. Delivery* **2016**, *7*, 101.
- [11] R. Mo, Z. Gu, *Mater. Today* **2016**, *19*, 274.
- [12] Q. Zhang, Z. Wu, N. Li, Y. Pu, B. Wang, T. Zhang, J. Tao, *Mater. Sci. Eng., C* **2017**, *77*, 1363.
- [13] M. Nejbat, F. Charbgo, M. Ramezani, *J. Biomed. Mater. Res., Part A* **2017**, *105*, 2355.
- [14] K. Yang, L. Feng, Z. Liu, *Adv. Drug Delivery Rev.* **2016**, *105*, 228.
- [15] E. Cabane, X. Zhang, K. Langowska, C. G. Palivan, W. Meier, *Biointerphases* **2012**, *7*, 9.
- [16] Y. Wang, Z. Li, D. Hu, C. T. Lin, J. Li, Y. Lin, *J. Am. Chem. Soc.* **2010**, *132*, 9274.
- [17] H. Chen, Z. Wang, S. Zong, L. Wu, P. Chen, D. Zhu, C. Wang, S. Xu, Y. Cui, *ACS Appl. Mater. Interfaces* **2014**, *6*, 17526.
- [18] C. Yao, Y. Tu, L. Ding, C. Li, J. Wang, H. Fang, Y. Huang, K. Zhang, Q. Lu, M. Wu, Y. Wang, *Bioconjug. Chem.* **2017**, *28*, 2608.
- [19] Y. Luo, X. Cai, H. Li, Y. Lin, D. Du, *ACS Appl. Mater. Interfaces* **2016**, *8*, 4048.
- [20] Y. Cao, H. Dong, Z. Yang, X. Zhong, Y. Chen, W. Dai, X. Zhang, *ACS Appl. Mater. Interfaces* **2017**, *9*, 159.
- [21] L. Deng, Q. Li, S. Al-Rehili, H. Omar, A. Almalik, A. Alshamsan, J. Zhang, N. M. Khashab, *ACS Appl. Mater. Interfaces* **2016**, *8*, 6859.
- [22] R. Garriga, I. Jurewicz, S. Seyedin, N. Bardi, S. Totti, B. Matta-Domjan, E. G. Velliou, M. A. Alkhorayef, V. L. Cebolla, J. M. Razal, A. B. Dalton, E. Munoz, *Nanoscale* **2017**, *9*, 7791.
- [23] H. Ding, F. Zhang, C. Zhao, Y. Lv, G. Ma, W. Wei, Z. Tian, *ACS Appl. Mater. Interfaces* **2017**, *9*, 27396.
- [24] M. Li, X. Yang, J. Ren, K. Qu, X. Qu, *Adv. Mater.* **2012**, *24*, 1722.
- [25] K. Yang, L. Hu, X. Ma, S. Ye, L. Cheng, X. Shi, C. Li, Y. Li, Z. Liu, *Adv. Mater.* **2012**, *24*, 1868.
- [26] Y. W. Chen, T. Y. Liu, P. H. Chang, P. H. Hsu, H. L. Liu, H. C. Lin, S. Y. Chen, *Nanoscale* **2016**, *8*, 12648.
- [27] C. Dai, S. Zhang, Z. Liu, R. Wu, Y. Chen, *ACS Nano* **2017**, *11*, 9467.
- [28] E. Peng, E. S. Choo, P. Chandrasekharan, C. T. Yang, J. Ding, K. H. Chuang, J. M. Xue, *Small* **2012**, *8*, 3620.
- [29] S. Hatamie, M. M. Ahadian, M. A. Ghiass, A. Iraj Zad, R. Saber, B. Parseh, M. A. Oghabian, S. Shanehsazzadeh, *Colloids Surf., B* **2016**, *146*, 271.
- [30] M. Hashemi, M. Omid, B. Muralidharan, H. Smyth, M. A. Mohagheghi, J. Mohammadi, T. E. Milner, *ACS Appl. Mater. Interfaces* **2017**, *9*, 32607.
- [31] Y. W. Chen, P. J. Chen, S. H. Hu, I. W. Chen, S. Y. Chen, *Adv. Funct. Mater.* **2014**, *24*, 451.
- [32] K. Yang, S. Zhang, G. Zhang, X. Sun, S. T. Lee, Z. Liu, *Nano Lett.* **2010**, *10*, 3318.
- [33] H. W. Liu, W. C. Huang, C. S. Chiang, S. H. Hu, C. H. Liao, Y. Y. Chen, S. Y. Chen, *Adv. Funct. Mater.* **2014**, *24*, 3715.
- [34] A. Servant, V. Leon, D. Jasim, L. Methven, P. Limousin, E. V. Fernandez-Pacheco, M. Prato, K. Kostarelos, *Adv. Healthcare Mater.* **2014**, *3*, 1334.
- [35] C. L. Weaver, J. M. LaRosa, X. Luo, X. T. Cui, *ACS Nano* **2014**, *8*, 1834.
- [36] S. Ganguly, D. Ray, P. Das, P. P. Maity, S. Mondal, V. K. Aswal, S. Dhara, N. C. Das, *Ultrason. Sonochem.* **2018**, *42*, 212.
- [37] L. He, S. Sarkar, A. Barras, R. Boukherroub, S. Szunerits, D. Mandler, *Chem. Commun.* **2017**, *53*, 4022.
- [38] Y. Wang, R. Huang, G. Liang, Z. Zhang, P. Zhang, S. Yu, J. Kong, *Small* **2014**, *10*, 109.
- [39] W. Fan, B. Yung, P. Huang, X. Chen, *Chem. Rev.* **2017**, *117*, 13566.
- [40] X. Zhu, H. Zhang, H. Huang, Y. Zhang, L. Hou, Z. Zhang, *Nanotechnology* **2015**, *26*, 365103.
- [41] G. Huang, X. Zhu, H. Li, L. Wang, X. Chi, J. Chen, X. Wang, Z. Chen, J. Gao, *Nanoscale* **2015**, *7*, 2667.
- [42] L. Chen, X. Zhong, X. Yi, M. Huang, P. Ning, T. Liu, C. Ge, Z. Chai, Z. Liu, K. Yang, *Biomaterials* **2015**, *66*, 21.
- [43] Z. Zhang, J. Wang, C. Chen, *Adv. Mater.* **2013**, *25*, 3869.
- [44] G. Tian, X. Zhang, Z. Gu, Y. Zhao, *Adv. Mater.* **2015**, *27*, 7692.
- [45] M. Tada, Y. Nakai, T. Sasaki, T. Hamada, R. Nagano, D. Mohri, K. Miyabayashi, K. Yamamoto, H. Kogure, K. Kawakubo, Y. Ito, N. Yamamoto, N. Sasahira, K. Hirano, H. Ijichi, K. Tateishi, H. Isayama, M. Omata, K. Koike, *World J. Clin. Oncol.* **2011**, *2*, 158.
- [46] R. Bayat Mokhtari, T. S. Homayouni, N. Baluch, E. Morgatskaya, S. Kumar, B. Das, H. Yeger, *Oncotarget* **2017**, *8*, 38022.
- [47] R. M. Webster, *Nat. Rev. Drug Discovery* **2016**, *15*, 81.
- [48] C. Zhang, T. Lu, J. G. Tao, G. Wan, H. X. Zhao, *RSC Adv.* **2016**, *6*, 15460.
- [49] J. A. Kemp, M. S. Shim, C. Y. Heo, Y. J. Kwon, *Adv. Drug Delivery Rev.* **2016**, *98*, 3.
- [50] W. Li, J. S. Wang, J. S. Ren, X. G. Qu, *Angew. Chem., Int. Ed.* **2013**, *52*, 6726.
- [51] G. Battogtokh, Y. T. Ko, *J. Controlled Release* **2016**, *234*, 10.
- [52] Y. Oh, J. Y. Je, M. S. Moorthy, H. Seo, W. H. Cho, *Int. J. Pharm.* **2017**, *531*, 1.
- [53] H. Kim, D. Lee, J. Kim, T. I. Kim, W. J. Kim, *ACS Nano* **2013**, *7*, 6735.
- [54] Y. Chen, P. F. Xu, Z. Shu, M. Y. Wu, L. Z. Wang, S. J. Zhang, Y. Y. Zheng, H. R. Chen, J. Wang, Y. P. Li, J. L. Shi, *Adv. Funct. Mater.* **2014**, *24*, 4386.
- [55] S. M. Sharker, J. E. Lee, S. H. Kim, J. H. Jeong, I. In, H. Lee, S. Y. Park, *Biomaterials* **2015**, *61*, 229.
- [56] S. M. Sharker, E. B. Kang, C. I. Shin, S. H. Kim, G. Lee, S. Y. Park, *J. Appl. Polym. Sci.* **2016**, *133*, 43791.
- [57] D. Y. Zhang, Y. Zheng, C. P. Tan, J. H. Sun, W. Zhang, L. N. Ji, Z. W. Mao, *ACS Appl. Mater. Interfaces* **2017**, *9*, 6761.
- [58] M. Hashemi, M. Omid, B. Muralidharan, L. Tayebi, M. J. Herpin, M. A. Mohagheghi, J. Mohammadi, H. D. C. Smyth, T. E. Milner, *Acta Biomater.* **2018**, *65*, 376.
- [59] S. Augustine, J. Singh, M. Srivastava, M. Sharma, A. Das, B. D. Malhotra, *Biomater. Sci.* **2017**, *5*, 901.
- [60] Y. Ma, Y. Ge, L. Li, *Mater. Sci. Eng., C* **2017**, *71*, 1281.
- [61] K. Yang, L. Feng, Z. Liu, *Expert Opin. Drug Delivery* **2015**, *12*, 601.
- [62] G. Reina, J. M. Gonzalez-Dominguez, A. Criado, E. Vazquez, A. Bianco, M. Prato, *Chem. Soc. Rev.* **2017**, *46*, 4400.

- [63] Y. Duan, C. D. Stinespring, B. Chorpeneing, *ChemistryOpen* **2015**, *4*, 642.
- [64] K. S. Novoselov, A. K. Geim, S. V. Morozov, D. Jiang, Y. Zhang, S. V. Dubonos, I. V. Grigorieva, A. A. Firsov, *Science* **2004**, *306*, 666.
- [65] F. D'Apuzzo, A. R. Piacenti, F. Giorgianni, M. Autore, M. C. Guidi, A. Marcelli, U. Schade, Y. Ito, M. W. Chen, S. Lupi, *Nat. Commun.* **2017**, *8*, 14885.
- [66] S. P. Jovanovic, Z. Syrgiannis, Z. M. Markovic, A. Bonasera, D. P. Kopic, M. D. Budimir, D. D. Milivojevic, V. D. Spasojevic, M. D. Dramicanin, V. B. Pavlovic, B. M. Todorovic Markovic, *ACS Appl. Mater. Interfaces* **2015**, *7*, 25865.
- [67] J. T. Robinson, S. M. Tabakman, Y. Liang, H. Wang, H. S. Casalongue, D. Vinh, H. Dai, *J. Am. Chem. Soc.* **2011**, *133*, 6825.
- [68] M. Choi, K. G. Kim, J. Heo, H. Jeong, S. Y. Kim, J. Hong, *Sci. Rep.* **2015**, *5*, 17631.
- [69] D. Yu, P. Ruan, Z. Meng, J. Zhou, *J. Pharm. Sci.* **2015**, *104*, 2489.
- [70] V. Georgakilas, J. A. Perman, J. Tucek, R. Zboril, *Chem. Rev.* **2015**, *115*, 4744.
- [71] X. Gao, Y. Wang, X. Liu, T. L. Chan, S. Irlé, Y. Zhao, S. B. Zhang, *Phys. Chem. Chem. Phys.* **2011**, *13*, 19449.
- [72] L. Yan, Y. B. Zheng, F. Zhao, S. Li, X. Gao, B. Xu, P. S. Weiss, Y. Zhao, *Chem. Soc. Rev.* **2012**, *41*, 97.
- [73] D. A. Dikin, S. Stankovich, E. J. Zimney, R. D. Piner, G. H. Dommett, G. Evmenenko, S. T. Nguyen, R. S. Ruoff, *Nature* **2007**, *448*, 457.
- [74] K. P. Loh, Q. L. Bao, P. K. Ang, J. X. Yang, *J. Mater. Chem.* **2010**, *20*, 2277.
- [75] D. R. Dreyer, S. Park, C. W. Bielawski, R. S. Ruoff, *Chem. Soc. Rev.* **2010**, *39*, 228.
- [76] S. H. Dave, C. Gong, A. W. Robertson, J. H. Warner, J. C. Grossman, *ACS Nano* **2016**, *10*, 7515.
- [77] F. Chen, N. J. Tao, *Acc. Chem. Res.* **2009**, *42*, 429.
- [78] X. Wan, K. Chen, D. Q. Liu, J. Chen, Q. Miao, J. B. Xu, *Chem. Mater.* **2012**, *24*, 3906.
- [79] V. Georgakilas, J. N. Tiwari, K. C. Kemp, J. A. Perman, A. B. Bourlinos, K. S. Kim, R. Zboril, *Chem. Rev.* **2016**, *116*, 5464.
- [80] K. T. Nguyen, Y. Zhao, *Nanoscale* **2014**, *6*, 6245.
- [81] P. T. Yin, S. Shah, M. Chowalla, K. B. Lee, *Chem. Rev.* **2015**, *115*, 2483.
- [82] Q. Li, N. Mahmood, J. H. Zhu, Y. L. Hou, S. H. Sun, *Nano Today* **2014**, *9*, 668.
- [83] Y. Jin, J. Wang, H. Ke, S. Wang, Z. Dai, *Biomaterials* **2013**, *34*, 4794.
- [84] X. D. Li, X. L. Liang, X. L. Yue, J. R. Wang, C. H. Li, Z. J. Deng, L. J. Jing, L. Lin, E. Z. Qu, S. M. Wang, C. L. Wu, H. X. Wu, Z. F. Dai, *J. Mater. Chem. B* **2014**, *2*, 217.
- [85] K. Turcheniuk, T. Dumych, R. Bilyy, V. Turcheniuk, J. Bouckaert, V. Vovk, V. Chopyak, V. Zaitsev, P. Mariot, N. Prevarskaya, R. Boukherroub, S. Szunerits, *RSC Adv.* **2016**, *6*, 1600.
- [86] H. I. Seo, Y. A. Cheon, B. G. Chung, *Biomed. Eng. Lett.* **2016**, *6*, 10.
- [87] G. Bottari, M. A. Herranz, L. Wibmer, M. Volland, L. Rodriguez-Perez, D. M. Guldi, A. Hirsch, N. Martin, F. D'Souza, T. Torres, *Chem. Soc. Rev.* **2017**, *46*, 4464.
- [88] V. Georgakilas, M. Otyepka, A. B. Bourlinos, V. Chandra, N. Kim, K. C. Kemp, P. Hobza, R. Zboril, K. S. Kim, *Chem. Rev.* **2012**, *112*, 6156.
- [89] X. Q. Ji, Y. H. Xu, W. L. Zhang, L. Cui, J. Q. Liu, *Composites, Part A* **2016**, *87*, 29.
- [90] D. Chen, H. Feng, J. Li, *Chem. Rev.* **2012**, *112*, 6027.
- [91] M. Veerapandian, Y. T. Seo, H. Shin, K. Yun, M. H. Lee, *Int. J. Nanomedicine* **2012**, *7*, 6123.
- [92] X. C. Qin, Z. Y. Guo, Z. M. Liu, W. Zhang, M. M. Wan, B. W. Yang, *J. Photochem. Photobiol., B* **2013**, *120*, 156.
- [93] X. W. Zheng, W. H. Chen, P. Cui, Z. M. Wang, W. Zhang, *RSC Adv.* **2014**, *4*, 58489.
- [94] M. Alibolandi, M. Mohammadi, S. M. Taghdisi, M. Ramezani, K. Abnous, *Carbohydr. Polym.* **2017**, *155*, 218.
- [95] P. Swietach, R. D. Vaughan-Jones, A. L. Harris, A. Hulikova, *Philos. Trans. R. Soc., B* **2014**, *369*, 20130099.
- [96] Y. Kato, S. Ozawa, C. Miyamoto, Y. Maehata, A. Suzuki, T. Maeda, Y. Baba, *Cancer Cell Int.* **2013**, *13*, 89.
- [97] Y. J. Zhu, F. Chen, *Chem. Asian J.* **2015**, *10*, 284.
- [98] L. Ren, T. Liu, J. Guo, S. Guo, X. Wang, W. Wang, *Nanotechnology* **2010**, *21*, 335701.
- [99] J. Liu, S. Guo, L. Han, W. Ren, Y. Liu, E. Wang, *Talanta* **2012**, *101*, 151.
- [100] L. Feng, K. Li, X. Shi, M. Gao, J. Liu, Z. Liu, *Adv. Healthcare Mater.* **2014**, *3*, 1261.
- [101] Z. Fan, S. Zhou, C. Garcia, L. Fan, J. Zhou, *Nanoscale* **2017**, *9*, 4928.
- [102] C. Shao, J. Liang, S. He, T. Luan, J. Yu, H. Zhao, J. Xu, L. Tian, *Anal. Chem.* **2017**, *89*, 5445.
- [103] L. Yue, J. Wang, Z. Dai, Z. Hu, X. Chen, Y. Qi, X. Zheng, D. Yu, *Bioconjugate Chem.* **2017**, *28*, 400.
- [104] R. J. Aitken, S. D. Roman, *Oxid. Med. Cell. Longevity* **2008**, *1*, 15.
- [105] K. B. Pandey, S. I. Rizvi, *Phytother. Res.* **2010**, *24*, S11.
- [106] O. Zitka, S. Skalickova, J. Gumulec, M. Masarik, V. Adam, J. Hubalek, L. Trnkova, J. Kruseova, T. Eckschlager, R. Kizek, *Oncol. Lett.* **2012**, *4*, 1247.
- [107] F. Jiang, A. M. Robin, M. Katakowski, L. Tong, M. Espiritu, G. Singh, M. Chopp, *Lasers Med. Sci.* **2003**, *18*, 128.
- [108] H. Xiong, Z. Guo, W. Zhang, H. Zhong, S. Liu, Y. Ji, *J. Photochem. Photobiol., B* **2014**, *138*, 191.
- [109] X. Zhao, L. Yang, X. Li, X. Jia, L. Liu, J. Zeng, J. Guo, P. Liu, *Bioconjugate Chem.* **2015**, *26*, 128.
- [110] K. Y. Yasoda, K. N. Bobba, D. Nedungadi, D. Dutta, M. S. Kumar, N. Kothurkar, N. Mishra, S. Bhuniya, *RSC Adv.* **2016**, *6*, 62385.
- [111] H. Wen, C. Dong, H. Dong, A. Shen, W. Xia, X. Cai, Y. Song, X. Li, Y. Li, D. Shi, *Small* **2012**, *8*, 760.
- [112] C. Alvarez-Lorenzo, A. M. Puga, A. Concheiro, *Nanostructures and Nanostructured Networks for Smart Drug Delivery*, Wiley-VCH, Weinheim, Germany **2012**, p. 417.
- [113] M. A. Keller, G. Piedrafito, M. Ralsler, *Curr. Opin. Biotechnol.* **2015**, *34*, 153.
- [114] Y. Xiong, K. L. Guan, *J. Cell Biol.* **2012**, *198*, 155.
- [115] F. Ding, F. H. Wu, Q. Q. Tian, L. L. Guo, J. Wang, F. H. Xiao, Y. Y. Yu, *RSC Adv.* **2016**, *6*, 68134.
- [116] S. Gao, L. Zhang, G. Wang, K. Yang, M. Chen, R. Tian, Q. Ma, L. Zhu, *Biomaterials* **2016**, *79*, 36.
- [117] Y. Cho, H. Kim, Y. Choi, *Chem. Commun.* **2013**, *49*, 1202.
- [118] J. H. van Ree, K. B. Jeganathan, L. Malureanu, J. M. van Deursen, *J. Cell Biol.* **2010**, *188*, 83.
- [119] K. Kessenbrock, V. Plaks, Z. Werb, *Cell* **2010**, *141*, 52.
- [120] C. O. McAtee, J. J. Barycki, M. A. Simpson, *Adv. Cancer Res.* **2014**, *123*, 1.
- [121] N. Aggarwal, B. F. Sloane, *Proteomics: Clin. Appl.* **2014**, *8*, 427.
- [122] M. Karimi, A. Ghasemi, P. Sahandi Zangabad, R. Rahighi, S. M. Moosavi Basri, H. Mirshekari, M. Amiri, Z. Shafaei Pishabad, A. Aslani, M. Bozorgomid, D. Ghosh, A. Beyzavi, A. Vaseghi, A. R. Aref, L. Haghani, S. Bahrami, M. R. Hamblin, *Chem. Soc. Rev.* **2016**, *45*, 1457.
- [123] R. Mo, T. Jiang, W. Sun, Z. Gu, *Biomaterials* **2015**, *50*, 67.
- [124] F. F. Zheng, P. H. Zhang, Y. Xi, J. J. Chen, L. L. Li, J. J. Zhu, *Anal. Chem.* **2015**, *87*, 11739.
- [125] D. He, X. He, K. Wang, Z. Zou, X. Yang, X. Li, *Langmuir* **2014**, *30*, 7182.

- [126] F. Li, S. Park, D. Ling, W. Park, J. Y. Han, K. Na, K. Char, *J. Mater. Chem. B* **2013**, *1*, 1678.
- [127] H. S. Jung, W. H. Kong, D. K. Sung, M.-Y. Lee, S. E. Beack, D. H. Keum, K. S. Kim, S. H. Yun, S. K. Hahn, *ACS Nano* **2014**, *8*, 260.
- [128] F. Nasrollahi, J. Varshosaz, A. A. Khodadadi, S. Lim, A. Jahani-Najafabadi, *ACS Appl. Mater. Interfaces* **2016**, *8*, 13282.
- [129] D. W. Hwang, H. Y. Kim, F. Li, J. Y. Park, D. Kim, J. H. Park, H. S. Han, J. W. Byun, Y. S. Lee, J. M. Jeong, K. Char, D. S. Lee, *Biomaterials* **2017**, *121*, 144.
- [130] T. Jiang, W. Sun, Q. Zhu, N. A. Burns, S. A. Khan, R. Mo, Z. Gu, *Adv. Mater.* **2015**, *27*, 1021.
- [131] M. G. Sikkandhar, A. M. Nedumaran, R. Ravichandar, S. Singh, I. Santhakumar, Z. C. Coh, S. Mishra, G. Archunan, B. Gulyas, P. Padmanabhan, *Int. J. Mol. Sci.* **2017**, *18*, 1036.
- [132] X. Li, J. Kim, J. Yoon, X. Chen, *Adv. Mater.* **2017**, *29*, 1606857.
- [133] R. Jahanban-Esfahlan, M. de la Guardia, D. Ahmadi, B. Yousefi, *J. Cell Physiol.* **2018**, *233*, 2019.
- [134] N. Tyagi, N. F. Attia, K. E. Geckeler, *J. Colloid Interface Sci.* **2017**, *498*, 364.
- [135] A. P. Blum, J. K. Kammeyer, A. M. Rush, C. E. Callmann, M. E. Hahn, N. C. Gianneschi, *J. Am. Chem. Soc.* **2015**, *137*, 2140.
- [136] A. Gulzar, S. L. Gai, P. P. Yang, C. X. Li, M. B. Ansari, J. Lin, *J. Mater. Chem. B* **2015**, *3*, 8599.
- [137] J. Yao, J. Feng, J. Chen, *Asian J. Pharm. Sci.* **2016**, *11*, 585.
- [138] D. Kishore, S. Kundu, A. M. Kayastha, *PLoS One* **2012**, *7*, e50380.
- [139] Z. Q. Wang, L. C. Ciacchi, G. Wei, *Appl. Sci.* **2017**, *7*, 1175.
- [140] L. Feng, L. Wu, X. Qu, *Adv. Mater.* **2013**, *25*, 168.
- [141] L.-Z. Bai, D.-L. Zhao, Y. Xu, J.-M. Zhang, Y.-L. Gao, L.-Y. Zhao, J.-T. Tang, *Mater. Lett.* **2012**, *68*, 399.
- [142] W. Legon, A. Rowlands, A. Opitz, T. F. Sato, W. J. Tyler, *PLoS One* **2012**, *7*, e51177.
- [143] N. Zhang, S. K. H. Chow, K. S. Leung, W. H. Cheung, *J. Orthop. Transl.* **2017**, *9*, 52.
- [144] G. Y. Wan, Y. Liu, B. W. Chen, Y. Y. Liu, Y. S. Wang, N. Zhang, *Cancer Biol. Med.* **2016**, *13*, 325.
- [145] K. T. Vo, K. K. Matthay, S. G. DuBois, *Clin. Sarcoma Res.* **2016**, *6*, 9.
- [146] P. A. Vasey, *Br. J. Cancer* **2003**, *89*, S23.
- [147] T. Ji, Y. Zhao, Y. Ding, G. Nie, *Adv. Mater.* **2013**, *25*, 3508.
- [148] L. Schaaaf, M. Schwab, C. Ulmer, S. Heine, T. E. Murdter, J. O. Schmid, G. Sauer, W. E. Aulitzky, H. van der Kuip, *Cancer Res.* **2016**, *76*, 2868.
- [149] X. Sun, G. Zhang, R. S. Keynton, M. G. O'Toole, D. Patel, A. M. Gobin, *Nanomedicine* **2013**, *9*, 1214.
- [150] Y. D. Livney, Y. G. Assaraf, *Adv. Drug Delivery Rev.* **2013**, *65*, 1716.
- [151] G. Tian, X. Zhang, X. Zheng, W. Yin, L. Ruan, X. Liu, L. Zhou, L. Yan, S. Li, Z. Gu, Y. Zhao, *Small* **2014**, *10*, 4160.
- [152] Y. Wang, K. Wang, J. Zhao, X. Liu, J. Bu, X. Yan, R. Huang, *J. Am. Chem. Soc.* **2013**, *135*, 4799.
- [153] X. Yao, Z. Tian, J. Liu, Y. Zhu, N. Hanagata, *Langmuir* **2017**, *33*, 591.
- [154] Z. Tian, X. Yao, K. Ma, X. Niu, J. Grothe, Q. Xu, L. Liu, S. Kaskel, Y. Zhu, *ACS Omega* **2017**, *2*, 1249.
- [155] X. Wang, J. Zhang, Y. Wang, C. Wang, J. Xiao, Q. Zhang, Y. Cheng, *Biomaterials* **2016**, *81*, 114.
- [156] R. Dou, Z. Du, T. Bao, X. Dong, X. Zheng, M. Yu, W. Yin, B. Dong, L. Yan, Z. Gu, *Nanoscale* **2016**, *8*, 11531.
- [157] X. Xu, J. Wang, Y. Wang, L. Zhao, Y. Li, C. Liu, *Nanomedicine* **2017**, *S1549*, 30093.
- [158] P. Wang, S. Chen, Z. Cao, G. Wang, *ACS Appl. Mater. Interfaces* **2017**, *9*, 29055.
- [159] C. Xu, D. Yang, L. Mei, Q. Li, H. Zhu, T. Wang, *ACS Appl. Mater. Interfaces* **2013**, *5*, 12911.
- [160] L. Shao, R. Zhang, J. Lu, C. Zhao, X. Deng, Y. Wu, *ACS Appl. Mater. Interfaces* **2017**, *9*, 1226.
- [161] S. Hu, R. Fang, Y. Chen, B. Liao, I. Chen, S. Chen, *Adv. Funct. Mater.* **2014**, *24*, 4144.
- [162] Y. L. Su, K. T. Chen, Y. C. Sheu, S. Y. Sung, R. S. Hsu, C. S. Chiang, S. H. Hu, *ACS Nano* **2016**, *10*, 9420.
- [163] G. Goncalves, M. Vila, M. T. Portoles, M. Vallet-Regi, J. Gracio, P. A. Marques, *Adv. Healthcare Mater.* **2013**, *2*, 1072.
- [164] T. A. Tabish, S. Zhang, P. G. Winyard, *Redox Biol.* **2017**, *15*, 34.
- [165] Y. Cho, Y. Choi, *Chem. Commun.* **2012**, *48*, 9912.
- [166] L. Yan, Y. N. Chang, W. Y. Yin, G. Tian, L. J. Zhou, X. D. Liu, G. M. Xing, L. N. Zhao, Z. J. Gu, Y. L. Zhao, *Biomater. Sci.* **2014**, *2*, 1412.
- [167] Y. P. Zeng, S. L. Luo, Z. Y. Yang, J. W. Huang, H. Li, C. Liu, W. D. Wang, R. Li, *J. Mater. Chem. B* **2016**, *4*, 2190.
- [168] Y. Wei, F. Zhou, D. Zhang, Q. Chen, D. Xing, *Nanoscale* **2016**, *8*, 3530.
- [169] J. Ge, M. Lan, B. Zhou, W. Liu, L. Guo, H. Wang, Q. Jia, G. Niu, X. Huang, H. Zhou, X. Meng, P. Wang, C. S. Lee, W. Zhang, X. Han, *Nat. Commun.* **2014**, *5*, 4596.
- [170] W. Miao, G. Shim, S. Lee, S. Lee, Y. S. Choe, Y. K. Oh, *Biomaterials* **2013**, *34*, 3402.
- [171] L. Zhou, L. Zhou, S. Wei, X. Ge, J. Zhou, H. Jiang, F. Li, J. Shen, *J. Photochem. Photobiol., B* **2014**, *135*, 7.
- [172] C. Wu, Q. He, A. Zhu, D. Li, M. Xu, H. Yang, Y. Liu, *ACS Appl. Mater. Interfaces* **2014**, *6*, 21615.
- [173] K. Habiba, J. Encarnacion-Rosado, K. Garcia-Pabon, J. C. Villalobos-Santos, V. I. Makarov, J. A. Avalos, B. R. Weiner, G. Morell, *Int. J. Nanomed.* **2016**, *11*, 107.
- [174] G. R. Chang, S. K. Li, F. Z. Huang, X. Z. Zhang, Y. H. Shen, A. J. Xie, *J. Mater. Sci. Technol.* **2016**, *32*, 753.
- [175] H. Chen, Y. Wang, Y. Yao, S. Qiao, H. Wang, N. Tan, *Theranostics* **2017**, *7*, 3781.
- [176] J. M. Shen, F. Y. Gao, L. P. Guan, W. Su, Y. J. Yang, Q. R. Li, Z. C. Jin, *RSC Adv.* **2014**, *4*, 18473.
- [177] K. Muthoosamy, I. B. Abubakar, R. G. Bai, H. S. Loh, S. Manickam, *Sci. Rep.* **2016**, *6*, 32808.
- [178] R. K. Thapa, J. H. Byeon, H. G. Choi, C. S. Yong, J. O. Kim, *Nanotechnology* **2017**, *28*, 295101.
- [179] T. H. Tran, H. T. Nguyen, T. T. Pham, J. Y. Choi, H. G. Choi, C. S. Yong, J. O. Kim, *ACS Appl. Mater. Interfaces* **2015**, *7*, 28647.
- [180] J. Tian, Y. Luo, L. Huang, Y. Feng, H. Ju, B. Y. Yu, *Biosens. Bioelectron.* **2016**, *80*, 519.
- [181] B. Jang, H. Kwon, P. Katila, S. J. Lee, H. Lee, *Adv. Drug Delivery Rev.* **2016**, *98*, 113.
- [182] H. Dong, W. Dai, H. Ju, H. Lu, S. Wang, L. Xu, S. F. Zhou, Y. Zhang, X. Zhang, *ACS Appl. Mater. Interfaces* **2015**, *7*, 11015.
- [183] F. Yin, K. Hu, Y. Chen, M. Yu, D. Wang, Q. Wang, K. T. Yong, F. Lu, Y. Liang, Z. Li, *Theranostics* **2017**, *7*, 1133.
- [184] L. Zhang, Z. Lu, Q. Zhao, J. Huang, H. Shen, Z. Zhang, *Small* **2011**, *7*, 460.
- [185] C. Wang, S. Ravi, U. S. Garapati, M. Das, M. Howell, J. MallelaMallela, S. Alwarapan, S. S. Mohapatra, S. Mohapatra, *J. Mater. Chem. B* **2013**, *1*, 4396.
- [186] F. Zhi, H. Dong, X. Jia, W. Guo, H. Lu, Y. Yang, H. Ju, X. Zhang, Y. Hu, *PLoS One* **2013**, *8*, e60034.
- [187] H. W. Yang, C. Y. Huang, C. W. Lin, H. L. Liu, C. W. Huang, S. S. Liao, P. Y. Chen, Y. J. Lu, K. C. Wei, C. C. Ma, *Biomaterials* **2014**, *35*, 6534.
- [188] Y. L. He, L. F. Zhang, Z. Z. Chen, Y. Liang, Y. S. Zhang, Y. L. Bai, J. Zhang, Y. F. Li, *J. Mater. Chem. B* **2015**, *3*, 6462.
- [189] Y. Zeng, Z. Yang, H. Li, Y. Hao, C. Liu, L. Zhu, J. Liu, B. Lu, R. Li, *Sci. Rep.* **2017**, *7*, 43506.
- [190] N. Alegret, A. Criado, M. Prato, *Curr. Med. Chem.* **2017**, *24*, 529.
- [191] J. Yu, X. Chu, Y. Hou, *Chem. Commun.* **2014**, *50*, 11614.
- [192] X. Yang, X. Zhang, Y. Ma, Y. Huang, Y. Wang, Y. Chen, *J. Mater. Chem.* **2009**, *19*, 2710.

- [193] A. Ramachandra Kurup Sasikala, R. G. Thomas, A. R. Unnithan, B. Saravanakumar, Y. Y. Jeong, C. H. Park, C. S. Kim, *Sci. Rep.* **2016**, 6, 20543.
- [194] X. Yao, X. Niu, K. Ma, P. Huang, J. Grothe, S. Kaskel, Y. Zhu, *Small* **2017**, 13, 1602225.
- [195] F. Wo, R. Xu, Y. Shao, Z. Zhang, M. Chu, D. Shi, S. Liu, *Theranostics* **2016**, 6, 485.
- [196] C. W. Song, H. J. Park, C. K. Lee, R. Griffin, *Int. J. Hyperthermia* **2005**, 21, 761.
- [197] P. Zhao, M. Zheng, Z. Luo, P. Gong, G. Gao, Z. Sheng, C. Zheng, Y. Ma, L. Cai, *Sci. Rep.* **2015**, 5, 14258.
- [198] K. N. Maloth, N. Velpula, S. Kodangal, M. Sangmesh, K. Vellamchetla, S. Ugrappa, N. Meka, *J. Lasers Med. Sci.* **2016**, 7, 30.
- [199] S. Wang, W. Fan, G. Kim, H. J. Hah, Y. E. Lee, R. Kopelman, M. Ethirajan, A. Gupta, L. N. Goswami, P. Pera, J. Morgan, R. K. Pandey, *Lasers Surg. Med.* **2011**, 43, 686.
- [200] R. R. Xing, T. F. Jiao, Y. M. Liu, K. Ma, Q. L. Zou, G. H. Ma, X. H. Yan, *Polymers* **2016**, 8, 181.
- [201] B. Tian, C. Wang, S. Zhang, L. Feng, Z. Liu, *ACS Nano* **2011**, 5, 7000.
- [202] G. Gollavelli, Y. C. Ling, *Biomaterials* **2014**, 35, 4499.
- [203] B. B. Fan, H. H. Guo, J. Shi, C. Y. Shi, Y. Jia, H. L. Wang, D. L. Chen, Y. J. Yang, H. X. Lu, H. L. Xu, R. Zhang, *J. Nanosci. Nanotechnol.* **2016**, 16, 7049.
- [204] Y. Wang, H. Wang, D. Liu, S. Song, X. Wang, H. Zhang, *Biomaterials* **2013**, 34, 7715.
- [205] A. Hervault, N. T. Thanh, *Nanoscale* **2014**, 6, 11553.
- [206] G. Chang, Y. Wang, B. Gong, Y. Xiao, Y. Chen, S. Wang, S. Li, F. Huang, Y. Shen, A. Xie, *ACS Appl. Mater. Interfaces* **2015**, 7, 11246.
- [207] E. J. Hong, D. G. Choi, M. S. Shim, *Acta Pharm. Sin. B* **2016**, 6, 297.
- [208] P. Huang, C. Xu, J. Lin, C. Wang, X. Wang, C. Zhang, X. Zhou, S. Guo, D. Cui, *Theranostics* **2011**, 1, 240.
- [209] Y. Meng, S. Wang, C. Li, M. Qian, X. Yan, S. Yao, X. Peng, Y. Wang, R. Huang, *Biomaterials* **2016**, 100, 134.
- [210] J. Kim, J. Kim, C. Jeong, W. J. Kim, *Adv. Drug Delivery Rev.* **2016**, 98, 99.
- [211] K. Bates, K. Kostarelos, *Adv. Drug Delivery Rev.* **2013**, 65, 2023.
- [212] A. Asokan, J. S. Johnson, C. Li, R. J. Samulski, *Gene Ther.* **2008**, 15, 1618.
- [213] R. Imani, W. Shao, S. Taherkhani, S. H. Emami, S. Prakash, S. Faghihi, *Colloids Surf., B* **2016**, 147, 315.
- [214] L. L. Ren, Y. F. Zhang, C. Y. Cui, Y. Z. Bi, X. Ge, *RSC Adv.* **2017**, 7, 20553.
- [215] Z. Wang, S. Li, M. Zhang, Y. Ma, Y. Liu, W. Gao, J. Zhang, Y. Gu, *Adv. Sci.* **2017**, 4, 1600327.
- [216] H. Kim, W. J. Kim, *Small* **2014**, 10, 117.
- [217] L. Feng, X. Yang, X. Shi, X. Tan, R. Peng, J. Wang, Z. Liu, *Small* **2013**, 9, 1989.
- [218] L. A. Emens, P. A. Ascierto, P. K. Darcy, S. Demaria, A. M. M. Eggermont, W. L. Redmond, B. Seliger, F. M. Marincola, *Eur. J. Cancer* **2017**, 81, 116.
- [219] M. Orecchioni, D. Bedognetti, F. Sgarrella, F. M. Marincola, A. Bianco, L. G. Delogu, *J. Transl. Med.* **2014**, 12, 138.
- [220] M. Orecchioni, C. Menard-Moyon, L. G. Delogu, A. Bianco, *Adv. Drug Delivery Rev.* **2016**, 105, 163.
- [221] A. Schinwald, F. A. Murphy, A. Jones, W. MacNee, K. Donaldson, *ACS Nano* **2012**, 6, 736.
- [222] G. Y. Chen, C. L. Chen, H. Y. Tuan, P. X. Yuan, K. C. Li, H. J. Yang, Y. C. Hu, *Adv. Healthcare Mater.* **2014**, 3, 1486.
- [223] H. Zhang, T. Yan, S. Xu, S. Feng, D. Huang, M. Fujita, X. D. Gao, *Mater. Sci. Eng., C* **2017**, 73, 144.
- [224] D. Yin, Y. Li, H. Lin, B. Guo, Y. Du, X. Li, H. Jia, X. Zhao, J. Tang, L. Zhang, *Nanotechnology* **2013**, 24, 105102.
- [225] X. Yu, D. Gao, L. Gao, J. Lai, C. Zhang, Y. Zhao, L. Zhong, B. Jia, F. Wang, X. Chen, Z. Liu, *ACS Nano* **2017**, 11, 10147.
- [226] M. J. Feito, M. Vila, M. C. Matesanz, J. Linares, G. Goncalves, P. A. Marques, M. Vallet-Regi, J. M. Rojo, M. T. Portoles, *J. Colloid Interface Sci.* **2014**, 432, 221.
- [227] Y. Tao, E. Ju, J. Ren, X. Qu, *Biomaterials* **2014**, 35, 9963.
- [228] J. Vollmer, A. M. Krieg, *Adv. Drug Delivery Rev.* **2009**, 61, 195.
- [229] R. F. Thompson, A. Maity, *Adv. Exp. Med. Biol.* **2014**, 772, 147.
- [230] X. Yi, K. Yang, C. Liang, X. Y. Zhong, P. Ning, G. S. Song, D. L. Wang, C. C. Ge, C. Y. Chen, Z. F. Chai, Z. Liu, *Adv. Funct. Mater.* **2015**, 25, 4689.
- [231] M. Zhou, Y. Chen, M. Adachi, X. Wen, B. Erwin, O. Mawlawi, S. Y. Lai, C. Li, *Biomaterials* **2015**, 57, 41.
- [232] X. Liu, X. Zhang, M. Zhu, G. Lin, J. Liu, Z. Zhou, X. Tian, Y. Pan, *ACS Appl. Mater. Interfaces* **2017**, 9, 279.
- [233] H. W. Yang, M. Y. Hua, T. L. Hwang, K. J. Lin, C. Y. Huang, R. Y. Tsai, C. C. Ma, P. H. Hsu, S. P. Wey, P. W. Hsu, P. Y. Chen, Y. C. Huang, Y. J. Lu, T. C. Yen, L. Y. Feng, C. W. Lin, H. L. Liu, K. C. Wei, *Adv. Mater.* **2013**, 25, 3605.
- [234] G. Lalwani, M. D'Agati, A. M. Khan, B. Sitharaman, *Adv. Drug Delivery Rev.* **2016**, 105, 109.
- [235] F. M. Tonelli, V. A. Goulart, K. N. Gomes, M. S. Ladeira, A. K. Santos, E. Lorencon, L. O. Ladeira, R. R. Resende, *Nanomedicine* **2015**, 10, 2423.
- [236] K. Yang, J. Wan, S. Zhang, Y. Zhang, S. T. Lee, Z. Liu, *ACS Nano* **2011**, 5, 516.
- [237] H. Lin, Y. Chen, J. Shi, *Chem. Soc. Rev.* **2018**, 47, 1938.
- [238] M. Rahman, M. Z. Ahmad, J. Ahmad, J. Firdous, F. J. Ahmad, G. Mushtaq, M. A. Kamal, S. Akhter, *Curr. Drug. Metab.* **2015**, 16, 397.
- [239] J. Y. Guo, B. Xia, E. White, *Cell* **2013**, 155, 1216.
- [240] W. L. Ng, Q. Huang, X. Liu, M. Zimmerman, F. Li, C. Y. Li, *Transl. Cancer Res.* **2013**, 2, 442.
- [241] D. K. Deda, K. Araki, *J. Braz. Chem. Soc.* **2015**, 26, 2448.
- [242] J. M. Dabrowski, B. Pucelik, A. Regiel-Futyr, M. Brindell, O. Mazuryk, A. Kyziol, G. Stochel, W. Macyk, L. G. Arnaut, *Coordin. Chem. Rev.* **2016**, 325, 67.
- [243] A. E. de Groot, S. Roy, J. S. Brown, K. J. Pienta, S. R. Amend, *Mol. Cancer Res.* **2017**, 15, 361.
- [244] J. Cao, H. An, X. Huang, G. Fu, R. Zhuang, L. Zhu, J. Xie, F. Zhang, *Nanoscale* **2016**, 8, 10152.
- [245] P. Kalluru, R. Vankayala, C. S. Chiang, K. C. Hwang, *Biomaterials* **2016**, 95, 1.
- [246] Z. W. Chen, Z. H. Li, J. S. Wang, E. G. Ju, L. Zhou, J. S. Ren, X. G. Qu, *Adv. Funct. Mater.* **2014**, 24, 522.